Climate Dynamics (2006) 26: 387–405
DOI 10.1007/s00382-005-0090-8

Andreas Pauling · Jürg Luterbacher · Carlo Casty
Heinz Wanner

Five hundred years of gridded high-resolution precipitation reconstructions over Europe and the connection to large-scale circulation

Received: 6 July 2005 / Accepted: 17 October 2005 / Published online: 20 December 2005

Abstract We present seasonal precipitation reconstructions for European land areas (30°W to 40°E/30–71°N; given on a 0.5°×0.5° resolved grid) covering the period 1500–1900 together with gridded reanalysis from 1901 to 2000 (Mitchell and Jones 2005). Principal component regression techniques were applied to develop this dataset. A large variety of long instrumental precipitation series, precipitation indices based on documentary evidence and natural proxies (tree-ring chronologies, ice cores, corals and a speleothem) that are sensitive to precipitation signals were used as predictors. Transfer functions were derived over the 1901–1983 calibration period and applied to 1500–1900 in order to reconstruct the large-scale precipitation fields over Europe. The performance (quality estimation based on unresolved variance within the calibration period) of the reconstructions varies over centuries, seasons and space. Highest reconstructive skill was found for winter over central Europe and the Iberian Peninsula. Precipitation variability over the last half millennium reveals both large interannual and decadal fluctuations. Applying running correlations, we found major non-stationarities in the relation between large-scale circulation and regional precipitation. For several periods during the last 500 years, we identified key atmospheric modes for southern Spain/northern Morocco and central Europe as representations of two precipitation regimes. Using scaled composite analysis, we show that precipitation extremes over central Europe and southern Spain are linked to distinct pressure patterns. Due to its high spatial and temporal resolution, this dataset allows detailed studies of regional precipitation variability for all seasons, impact studies on different time and space scales, comparisons with high-resolution climate models as well as analysis of connections with regional temperature reconstructions.

Electronic Supplementary Material Supplementary material is available for this article at http://dx.doi.org/10.1007/s00382-005-0090-8 and is accessible for authorized users.

A. Pauling (✉) · J. Luterbacher · H. Wanner
Institute of Geography, University of Bern,
Hallerstrasse 12, CH-3012 Bern, Switzerland
E-mail: pauling@giub.unibe.ch
Tel.: +41-31-6318868
Fax: +41-31-6318511

J. Luterbacher · H. Wanner
National Center of Competence in Research (NCCR) in Climate,
Erlachstrasse 9a, CH-3012 Bern, Switzerland

C. Casty
Climate and Environmental Physics, Physics Institute,
University of Bern, Sidlerstrasse 5, CH-3012 Bern, Switzerland

1 Introduction

To detect anthropogenic warming, knowledge concerning the range of variability in hydroclimatic variables such as seasonal precipitation and drought in past centuries at regional and continental scale is important from a societal as well as scientific point of view (e.g. Jones and Mann 2004; Xoplaki et al. 2004; Touchan et al. 2003, 2005). Alongside temperature, precipitation is the key climatic factor affecting human economies and terrestrial ecosystems. Further, extreme precipitation events such as floods and droughts have an essential influence on human life (e.g. Cook et al 2004; Wanner et al. 2004; Barriendos 2005). Therefore, efforts should be made to increase our understanding of long-term changes in precipitation and drought patterns and their links to controlling circulation influences (e.g. Casty et al. 2005a; Hirschboeck 1988; Jacobeit et al. 2003; Jones and Mann 2004; Touchan et al. 2005; Wanner et al. 2004; Xoplaki et al. 2000, 2004). Also, the positive feedback mechanism between increased temperatures during the last few decades and an enhanced water cycle could be regionally studied on much longer timescales (IPCC 2001). Climatic reconstructions covering the last few centuries, however, require a dense network of suitable proxies. Europe is one of the few regions with substantial coverage of long instrumental records, documentary evidence and spatio-temporally highly resolved natural proxies.

Up to the present, continuous European precipitation reconstructions covering the last few centuries are only available for various regions such as south-east Germany (Wilson et al. 2005), southern Moravia, Czech Republic (Brázdil et al. 2002), Central Scandinavia (Linderholm and Chen 2005), Iberian Peninsula (Barriendos and Rodrigo 2005), southern Spain (Rodrigo et al. 1999, 2001), northwestern Spain (Saz 2004), southeastern Mediterranean (Touchan et al. 2003, 2005), the Alpine region (Casty et al. 2005a), parts of Tyrol, Austria (Oberhuber and Kofler 2002), western France (Masson-Delmotte et al. 2005; Raffalli-Delerce et al. 2004), Hungary (Rácz 1999), Switzerland (Pfister 1999; Gimmi et al. 2005), Germany (Glaser 2001), Sicily (Diodato 2006), Morocco (Till and Guiot 1990), southern Jordan (Touchan 1999), central Turkey (D'Arrigo and Cullen 2001; Akkemik and Aras 2005), western Black Sea region of Turkey (Akkemik et al. 2005) and the Canary Islands (García-Herrera et al. 2003).

This study aims at providing temporally and spatially highly resolved precipitation reconstructions hitherto not available. The new independently reconstructed precipitation fields will complement the existing reconstructions of other climatic variables such as surface air temperature (Luterbacher et al. 2004; Xoplaki et al. 2005), sea level pressure (SLP) and 500 hPa geopotential height fields (Luterbacher et al. 2002a; Casty et al. 2005c) for the Eastern North Atlantic/European area and will allow extensive analyses of European climate over the last 500 years. For the first time it is possible to perform such analyses on continental and regional scales.

Using this new precipitation dataset we examine the stationarity of the relationship of winter precipitation and atmospheric modes. Further, we investigate large-scale circulation that has led to extremely dry and extremely wet winters over Europe as well as over selected subregions where skilful reconstructions are achieved (see below).

This work is structured as follows: Sect. 2 describes the predictor and predictand data. It also outlines the reconstruction and verification methods. Additionally, an overview of running correlations and the scaled composite technique is given. Section 3 presents the reconstructions and their quality. They are compared with independent precipitation reconstructions and their connection to large-scale circulation is investigated. In Sect. 4 the results are discussed and in Sect. 5 conclusions are provided.

2 Data and methods

2.1 Predictor data

Three data types are used as predictors: long quality-checked instrumental precipitation series, precipitation indices based on documentary evidence and natural proxies (tree-ring chronologies, ice cores, corals and a speleothem) resolving precipitation signals. There are a few long instrumental precipitation series (e.g. Slonosky 2002; Wales-Smith 1971; Gimmi et al. 2005; Tabony 1981; Wigley et al. 1984; Camuffo 1984; Tarand 1993) while a few documentary indices date back as far as 1500 (see Fig. 1, lower panel). Documentary evidence comprises all non-instrumental man-made data on past weather and climate as well as instrumental observations prior to the set-up of continuous meteorological networks (e.g. Brázdil et al. 2005 and references therein; Pfister 2005; Przybylak et al. 2005). Non-instrumental evidence is subdivided into descriptive documentary data (including weather observations, e.g. reports from chronicles, daily weather reports, travel diaries, ship logbooks, etc.) and documentary proxy data (more indirect evidence that reflects weather events or climatic conditions such as the beginning of agricultural activities, religious ceremonies in favour of ending meteoro-

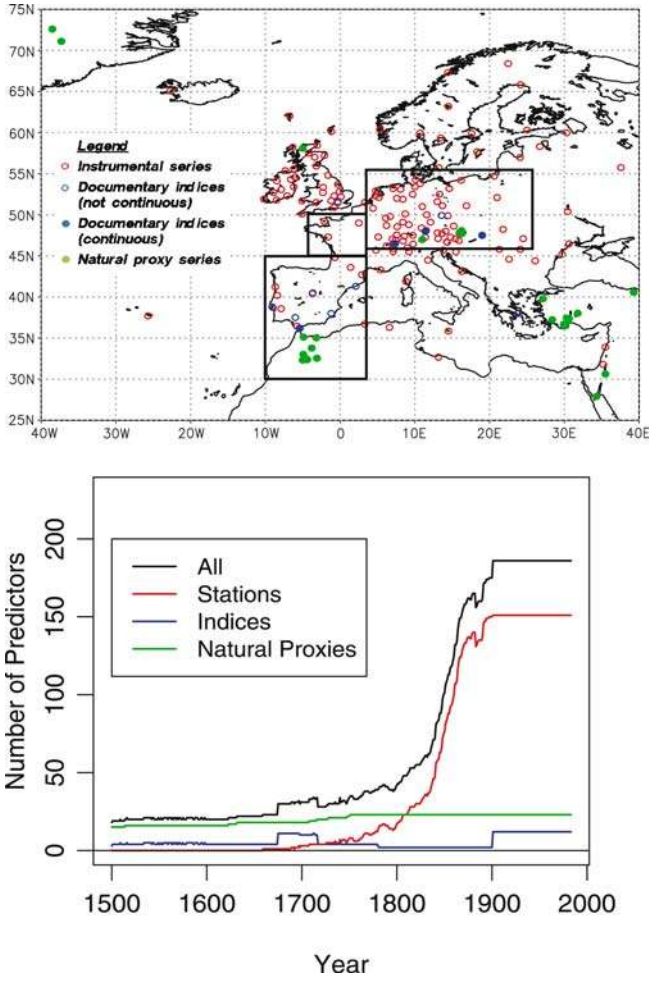

Fig. 1 Upper panel: spatial distribution and types of the proxies used for the Europe-wide precipitation reconstruction. The *rectangles* indicate the extent of the three regional reconstructions, which are discussed in more detail in the text. Lower panel: the temporal evolution of the number of proxies available for the winter reconstructions

logical stress such as drought or wet conditions, etc.) (e.g. Brázdil et al. 2005 and references therein; Pfister 2005; Barriendos 2005). The first step in the procedure to obtain indexed values is the evaluation of available documentary data taking into consideration the critical analysis of sources, author and/or institutional framework, calibration of documentary proxy data, etc. Useful values from documentary evidence are obtained by transforming the basic data into simple and weighted precipitation indices on an ordinal scale. Simple monthly indices use a three-term classification (precipitation: 1 wet, 0 normal, -1 dry with respect to a defined reference period within the 20th century). Seasonal indices are obtained by summation of monthly values. Therefore, in simple indices the 3-month seasonal values (e.g. DJF, MAM, JJA, and SON) can fluctuate from –3 (very dry) to 3 (very wet) (see Brázdil et al. 2005 for a detailed descripition). Series of indices obtained from documentary evidence should overlap the period of instrumental measurements. This is only possible for a few cases and very distinct periods (e.g. Pauling et al. 2003). In order to extend the historical indices into the 20th century, measurements have been indexed using the same numerical scheme (typically from -3 to +3) as the historical documentary indices. However, these measurement-derived indices from the 20th century probably overestimate the accuracy of the documentary series. In order to deal with this issue, white noise has been added to the measurement-derived indices. We have chosen white noise since the inaccuracies of two interannual seasonal documentary indices are believed to be uncorrelated. This degrading procedure has also been applied by Mann and Rutherford (2002), Pauling et al. (2003), Xoplaki et al. (2005) and Luterbacher et al. (2005) and is thought to model the inaccuracies present in the documentary indices. To estimate the magnitude of the added noise, an overlap period is needed. However, there are few examples where instrumental measurements and documentary indices are available for the same period (e.g. Brázdil and Friedmannová 1994 and Brázdil et al. 2003 both for the Czech Republic; Rácz 1999 for Hungary; Rodrigo et al. 1999 for Spain). Correlation coefficients between documentary indices and measurements in these studies vary and are of the order 0.5. The standard deviation of the added noise has been chosen to ensure to same correlation as in these studies.

Apart from documentary indices, natural proxies have been used. The tree-ring chronologies consist of networks that have been published for their seasonal precipitation signal (for the number and location see Fig. 1). However, some tree-rings are sensitive to winter precipitation, others to spring or summer precipitation. A list of all chronologies can be found in the electronic supplementary material accompanying this work. From this list it can also be seen for which season each chronology has been used as predictor. The applied standardization procedure included the following steps: By detrending and indexing (standardizing) the tree-ring measurement series, chronologies have been produced. Subsequently, a robust estimation of the mean value function is applied to remove effects of endogenous stand disturbances (ITRDB 2005). In many cases this has been done using the program ARSTAN (Cook and Holmes 1986). Standardization has a large effect on the frequency spectrum of the reconstructions. Here a procedure has been used that stresses interannual to interdecadal variability. Thus, lower frequencies of the reconstructions stem from other predictors than tree-rings.

Only those chronologies that start before 1750 and end after 1982 have been used to ensure full coverage of the calibration and verification period (1901–1983) as well as parts of the reconstruction period (1500–1900). The end date of the calibration (1983) has been chosen as a result of many natural proxies that end in the early 1980s. Additionally, to select the chronologies containing the strongest regional precipitation signal, backward elimination techniques (e.g. Luterbacher et al. 2005; Pauling et al. 2003; Ryan 1997) have been applied to these data. This method ranks the predictors according to the proportion of the predictand's variance they can explain. Subsequently, we removed iteratively the least important chronologies until the remaining chronologies still explained 90% of the seasonal variance that the full set of chronologies explained.

Four reconstructions have been performed (see rectangles in Fig. 1): one for European land areas (30°W to 40°E/30–71°N; hereafter ''European reconstruction'') as well as three regional reconstructions as there are different precipitation regimes over Europe (e.g. Qian et al. 2000; Zveryaev 2004): central-eastern Europe (3–25°E/46–56°N; hereafter CEE), France (5°W to 3°E/44–50°N; FRA) and the Iberian Peninsula including Morocco (10°W to 3°E/30–44°N; IPM). The advantage of the regional reconstructions is the slightly higher reconstructive skill. However, regional reconstructions are only possible where sufficient meaningful local predictors are available, as it is often impossible to rely on precipitation signals from remote regions for precipitation reconstructions. Therefore, we expanded the predictor sets for the regional reconstructions with further chronologies from the International Tree-ring Data Bank (ITRDB). From these chronologies only those that fulfil the same length requirements as above and correlate significantly with precipitation from the nearest grid point over the 1901–1983 period have been considered.

As the ice core records are not numerous, no rigorous selection could be performed. The Crete and the GISP ice core were selected because they have a high temporal resolution and are publicly available. Both ice cores are located on the ice divide of the Greenland ice cap. The parameters include annual accumulation rates, seasonal δH and δ^{18}O. Due to the high resolution of these ice cores it was possible to distinguish between winter and summer signals. The rationale for using these predictors is the known teleconnections between European and Greenland climate, especially during wintertime (e.g.

van Loon and Rogers 1978; Hurrell and van Loon 1997). These teleconnections are also confirmed by correlations of ~0.3 over the 1902–1990 period (significant at the 95% level) between ice core parameters and precipitation over various European regions (Spain, Scotland and north-eastern Europe).

Additionally, $\delta^{18}O$ from the bimonthly-resolved Ras Umm Sidd coral from the Red Sea (Felis et al. 2000) was used. The high resolution of this coral allowed to extract distinct seasonal climate signals. According to Felis et al. (2000) variations of coral $\delta^{18}O$ reflects both sea surface temperature and $\delta^{18}O$ of the seawater. They argue that colder conditions over the Red Sea is connected to increased rainfall in the southeastern Mediterranean basin and obtained a correlation coefficient of 0.36 (significant at the 99.5% level) between the mean annual coral $\delta^{18}O$ record and precipitation from Cairo. Further, they also report on oscillations in the coral $\delta^{18}O$ series that are probably due to the North Atlantic Oscillation (NAO)/Arctic Oscillation (AO) (Rimbu et al. 2001).

Finally, an annually dated speleothem from Scotland (Proctor et al. 2000) was used. This speleothem has also been shown to record precipitation throughout the year. Proctor et al. (2000) obtained a clear negative correlation of –0.53 over the 1879–1990 period (significant at the 99.9% level) between decadal smoothed data of bandwidth and annual local precipitation. According to Proctor et al. (2000) the cave of that stalagmite is located under a peat layer. They argue that CO_2 production in the overlying peat is quicker in warmer and drier conditions. The partial pressure of CO_2 in the drip water also determines the Ca^{2+} concentration, which in turn determines the growth rate of the speleothem making it a precipitation (and temperature) proxy. The annual dating was achieved through luminescent organic matter that form annual bands (Proctor et al. 2000). A list of all predictors can be found in the electronic supplementary material.

2.2 Predictand data

The gridded precipitation field by Mitchell and Jones (2005) was used as the dependent variable (predictand). This dataset has been developed by interpolating many instrumental precipitation station series onto a 0.5°×0.5° grid. It covers all global land areas 1901–2002. The values are expressed as anomalies from the 1961–1990 reference period. From this dataset we extracted the predictand for both the European and the four regional reconstructions.

2.3 Methods

2.3.1 Calibration

We aim at reconstructing gridded precipitation over Europe through multivariate statistical climate fields reconstruction (CFR) approaches (Jones and Mann 2004; Luterbacher et al. 2004; Brönnimann and Luterbacher 2004; Casty et al. 2005a,c; Rutherford et al. 2005; Xoplaki et al. 2005; Mann et al. 2005). CFR seeks to reconstruct large-scale climate patterns, such as precipitation, by assimilating a spatial network of proxy indicators. This so-called 'upscaling' involves fitting statistical models, which are mostly regression-based, between the local proxy/instrumental data and the large-scale climate fields/patterns. We perform a multivariate calibration of the large-scale information in the proxy data network against the available instrumental data under the assumption of stationarity. Principal component regression (PCR) has been used to perform the reconstructions. We retained 70% of the predictor's and 90% of the predictand's variance. A description of this technique can be found, e.g. in Jones and Mann (2004) and Luterbacher et al. (2002a, 2004).

First, all selected precipitation proxies in the European/North Atlantic region have been calibrated against a European precipitation field to produce the European reconstruction. Second, the three regional reconstructions were performed. For these regional reconstructions only predictors within the predictand field were used since remote predictors did not prove to be meaningful for precipitation in these regions. Reconstructive skill of the regional reconstructions is slightly higher compared with the European reconstruction (Figs. 3, 4). The 1901–1956 period has been used for calibration and the derived models have been verified using the data of the 1957–1983 period. Data after 1983 could not be used as many proxy series end at that time. Additionally, the calibration period could not be extended back into the 19th century as the Mitchell and Jones (2005) dataset starts in 1901. Therefore, the 1901–1983 period was used for calibration to reconstruct precipitation back to 1500.

2.3.2 Verification

The skill of the reconstructions has been estimated using the reduction of error (RE) measure (see review in Cook et al. 1994). It is defined as:

$$\mathrm{RE} = 1 - \frac{\sum_{i=i}^{n} (x_i - \hat{x}_i)^2}{\sum_{i=i}^{n} (x_i - \bar{x})^2},$$

where x_i are the observed values over the 1957–1983 *verification* period, $\hat{x}_i$ are the reconstructed values over the 1957–1983 *verification* period and $\bar{x}$ is the mean of the observed values over the 1901–1956 *calibration* period.

RE values of 1 indicate a perfect reconstruction (no difference between reconstruction and the predictand during the verification period), a value of 0 means that the reconstruction is as good as climatology (mean over the verification period) and –1 is equivalent to a random

guess. Thus, RE values larger than 0 indicate reconstructive skill. Due to the change of the predictors through time, we had to calibrate and verify numerous statistical models. For RE calculation of a certain model, we performed calibration (1901–1956) and verification (1957–1983) during the 20th century using the same predictors that are available for the period to be reconstructed (e.g. Luterbacher et al. 1999, 2002a, 2004; Xoplaki et al. 2005; Casty et al. 2005a). The assumption is, that the calculated RE within the verification period is also valid for the considered reconstruction period. Additionally to this measure, the reconstructions were compared with existing precipitation reconstructions that are independent from ours for further verification.

It is important to note that statistical reconstructions are always associated with uncertainties. In most cases, predictors can only explain parts of the predictand's variance. The unexplained part is the main source of the uncertainties in the reconstructions. Hence, we have calculated error ranges based on the predictor's variance not captured by the model. Similar to Briffa et al. (2002) we used ± 2 standard errors to provide an estimate of the uncertainties that are associated with the reconstructions. Thus, the uncertainty range of any reconstructed value is given by the equation:

$$\text{Uncertainty range} = v \pm 2\sqrt{\text{var}_{\text{unex}}}.$$

Where v is any reconstructed value and var_{unex} is the unexplained variance of a specific statistical model. According to Briffa et al. (2002) the uncertainty ranges are in fact timescale-dependent. The uncertainties presented here are only valid for individual values (i.e. seasons) rather than decadal or lower frequencies. Those uncertainties, however, do not take into account uncertainties in the instrumental precipitation data against which the multiproxy data are calibrated, nor the possibility of additional uncertainties in the proxy data prior to the calibration/verification periods (e.g. Jones and Mann 2004). The former are generally negligible compared to other contributions to uncertainty (e.g. Folland et al. 2001). The latter contribution may in some cases be large, suggesting circumspect use. In the case of tree-ring series that represent a composite of a decreasing number of contributing trees in the chronologies back in time or of documentary proxy data when earlier information is less reliable than the instrumental data (Jones and Mann 2004).

2.3.3 *Running correlations*

To investigate the stability of relations of climatic variables, running correlations are often used in climate research (e.g. Casty et al. 2005a; Gershunov et al. 2001; Jacobeit et al. 2001, 2003; Jones et al. 2003; Luterbacher et al. 1999; Schmutz et al. 2000; Slonosky and Yiou 2002; Slonosky et al. 2001b; Timm et al. 2004; Touchan et al. 2005). This technique includes calculation of correlation coefficients using a time window that is moved by one time unit over the whole time series. A 30-year running correlation analysis (ranging from 1500 to 2000) is performed to examine the relationship between winter precipitation averaged over the regions southern Spain/Morocco and Central Europe and large-scale atmospheric modes. These modes are defined as the three leading empirical orthogonal functions (EOFs) derived from a pressure dataset that has been reconstructed as described by Luterbacher et al. (2002a). The used version of the pressure reconstructions, however, rely solely on pressure and temperature information as predictors. Thus, they are independent from the precipitation reconstructions presented in this study (i.e. they share no common predictors).

There are small lag-one autocorrelations in the precipitation data. Gershunov et al. (2001) state that autocorrelations have to be accounted for when calculating significance thresholds. Therefore, to obtain a conservative estimate of significant correlations, we estimated 95% confidence levels using Monte-Carlo simulations. Thousand random time series having the same standard deviation, mean and lag-one autocorrelation coefficients as the original data are computed and then correlated (Wilks 1995).

2.3.4 *Scaled composites*

We have also used scaled composite analysis (Brown and Hall 1999; Touchan et al. 2005) to explore the relationship between precipitation extremes and the associated atmospheric patterns. Conventional composite analysis includes averaging a subset of the data, commonly extremes. According to Brown and Hall (1999) these analyses have at least two shortcomings: first, the mean is strongly influenced by outliers especially in small samples and second, it does not account for the associated variance. Therefore, we used scaled composites, which do not have these disadvantages as they are scaled to the square root of the sample size divided by the standard deviation. This method can also be applied to data that are not normally distributed (Brown and Hall 1999). The significance of the anomalies is assessed by modified t-values that account for the non-Gaussian distribution of the data (Brown and Hall 1999).

The scaled composites are based on the 5% wettest (25 cases) and the 5% driest (25 cases) winters (DJF) of the period 1500–2000. For these extreme winters we calculated the associated SLP anomalies and compared them with the scaled composites.

3 Results

3.1 Precipitation reconstructions

Figure 2 shows the spatially averaged time series of the European reconstruction. This provides an overview of the seasonal precipitation evolution over the last

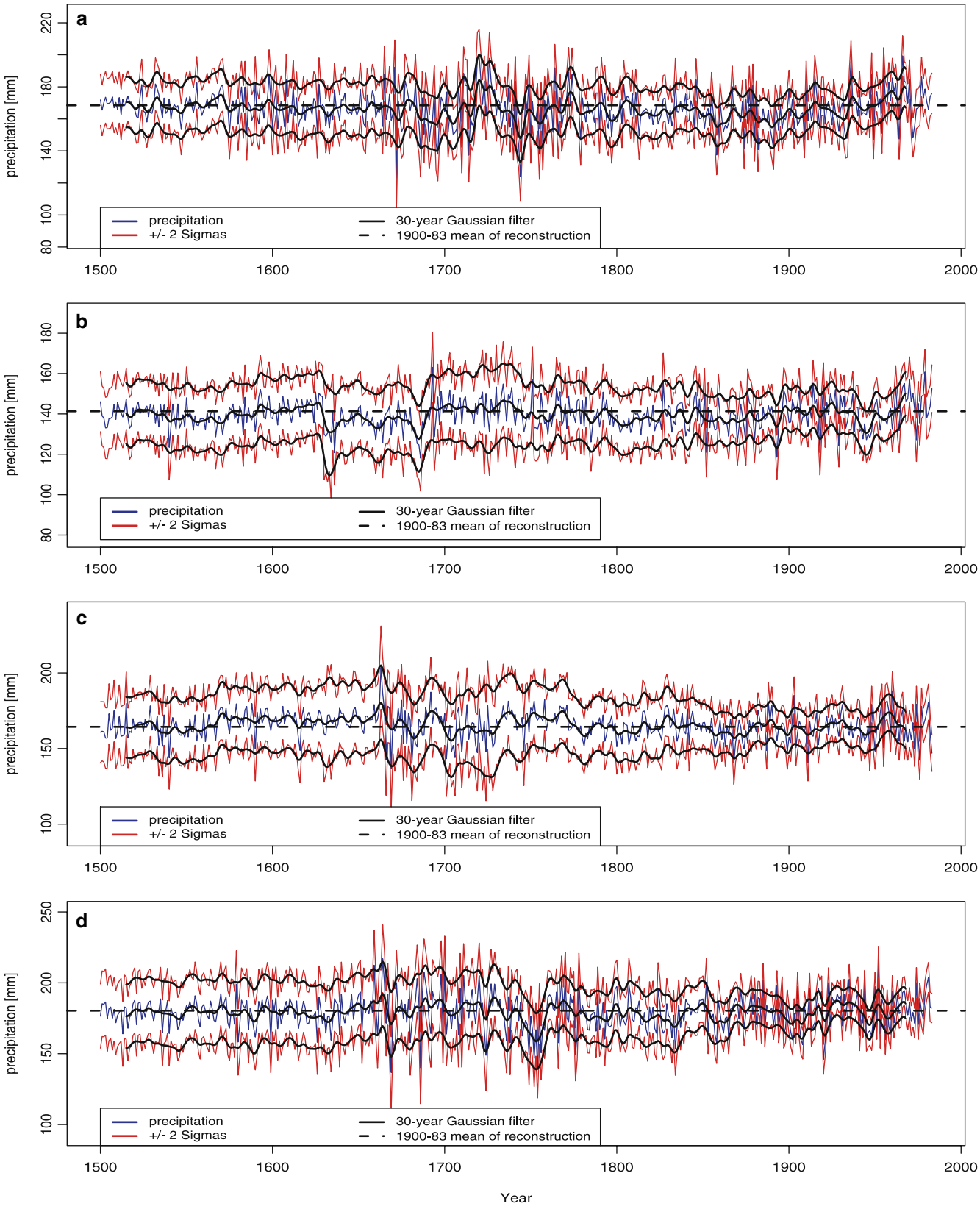

Fig. 2 Spatially averaged time series and uncertainty estimates of the European reconstruction. They are the average of the field 30°W to 40°E/30–71°N (5,791 land grid points). To the original reconstruction (*blue curve*) and its uncertainties (*red curves*) a 30-year-Gauss-filter is applied to stress the interdecadal fluctuations. The smoothed version is no new reconstruction and therefore the smoothed uncertainties can merely be interpreted as the general course of the interannual uncertainties and do not provide uncertainty estimates on decadal timescales (Sect. 2.3.2). a = winter (DJF), b = spring (MAM), c = summer (JJA), and d = autumn (SON)

500 years. However, we have also performed detailed spatial analysis of the precipitation history (Sect. 3.4.2). Beside trend analyses, additional time series of the regional reconstructions covering all seasons are provided in the electronic supplementary material.

The winter (DJF) reconstruction (Fig. 2a) is rather stable from 1500 to 1700. Thereafter, interdecadal variability increases with a sharp rise during approximately 1705–1720. This is followed by a pronounced decline during the following two decades to the lowest overall values. A second positive peak is reached around 1770. During the 19th century a slow decrease can be observed and the 20th century is characterized by a positive trend. The wettest winter on record is 1720 when precipitation reached around 200 mm. The dry counterpart occurred in 1744 with only 124 mm of precipitation. During the period 1500–1700, the unfiltered uncertainty amounts to approximately 35 mm. Afterwards, a gradual decrease can be observed to values of 25–30 mm in the 20th century.

Spring (MAM) precipitation (Fig. 2b) shows a steady increase from 1540 to around 1620. Thereafter, multidecadal variability increases until 1700. The first half of the 18th century is characterized by rather stable but above average precipitation levels. This is followed by a decline until 1800. The following 180 years show a gradual increase with a short period of rather low precipitation around 1950. Spring precipitation extremes occur during the second half of the 17th century: The year 1686 is the driest (118 mm) and 1693 the wettest (163 mm) spring on record. During 1500–1750 the uncertainty amounts to approximately 35 mm. After 1750 the uncertainty considerably decreases to values of around 25 mm. In the course of the 19th century the uncertainty reaches the same level as during the 20th century (20 mm) with similar variability.

Summer (JJA) precipitation (Fig. 2c) from 1500 to 1660 is characterized by a gradual increase. During the following 100 years, high decadal variability can be observed. From 1800 to 1983 variability decreases with

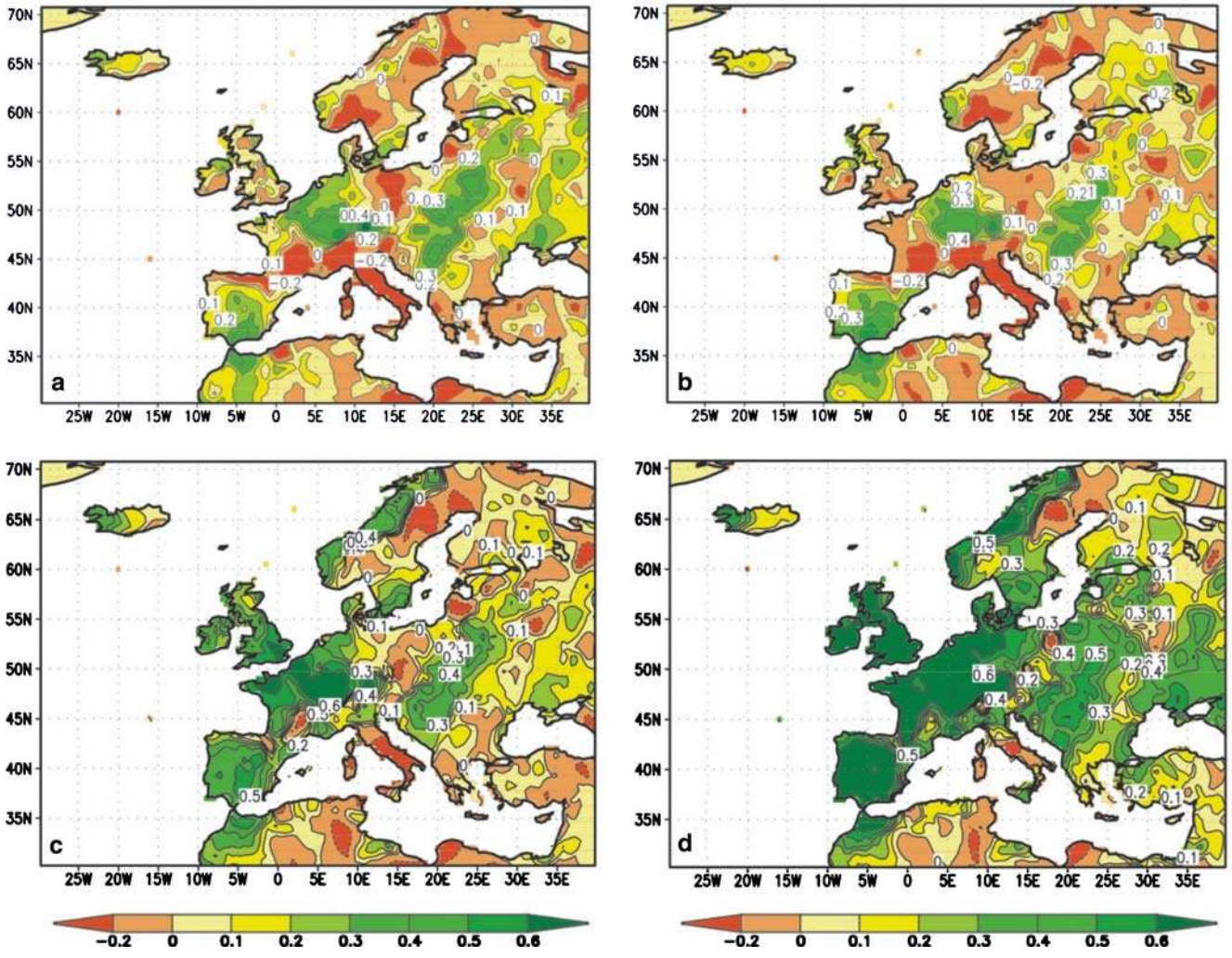

Fig. 3 Spatial distribution of the RE values for the European winter reconstruction for (**a**) 16th century, (**b**) 17th century, (**c**) 18th century and (**d**) 19th century

no overall trends. Extremely dry summers occur in 1666 (142 mm) and 1669 (137 mm) while 1663 (204 mm) is the wettest summer on record. The uncertainties remain the same from 16th to 18th century (40 mm) but decrease slightly after 1800 (35 mm) and reach values around 25 mm in 1900.

Autumn (SON) precipitation reveals no decadal variability and no trend from 1500 to around 1650. Thereafter, strong decadal fluctuations can be observed. Around 1800, however, variability is dominated by high frequencies and again reveals no obvious trend. The wettest autumn on record is reached in 1664 (217 mm), followed by the driest one in 1669 (137 mm). The uncertainty of this reconstruction remains rather stable until 1750 (40 mm) when it gradually decreases until 1860 when it reaches the level of the 20th century (20 mm).

The CEE reconstruction shows similar features as the European reconstruction. Together with the FRA and IPM reconstructions it is available in the electronic supplementary material.

3.2 Performance of the reconstructions

Figure 3 presents the RE values from the European reconstruction averaged over each century for winter. Similar figures for the other seasons can be found in the electronic supplementary material including analyses on the reconstructive skill of instrumental measurements relative to proxy data. In general, an increase from the 16th to the 19th century can be observed. This coincides with a steady increase of the number of available predictor information (Fig. 1). However, already in the 16th century there are regions with REs over 0.6 while neighbouring regions show no skill. During the 16th and 17th century regions with positive RE values for winter precipitation include central and eastern Europe, parts of the Iberian Peninsula and adjacent Morocco. During the 18th century RE values are above zero over western Europe including northern Morocco, parts of Scandinavia and eastern Europe. During the 19th century this pattern stays the same with RE values generally above the level of the 18th century.

Figure 4 shows the spatial distribution of the RE values of the CEE reconstruction for winter. During the 16th and 17th century reconstructive skill varies substantially within the study area. RE values range from below -0.2 to over 0.6 on relatively small spatial scales. In the 18th century most of western Europe and large parts of eastern Europe exhibit high reconstructive skill and during the 19th century RE values are over 0.6 in many parts of Europe. Compared with Fig. 3 those values are slightly higher. That feature is even more pronounced for the FRA reconstruction (see electronic supplementary material). RE maps for spring, summer and autumn reconstructions are also available from the electronic supplementary material. Generally, these reconstructions show somewhat lower

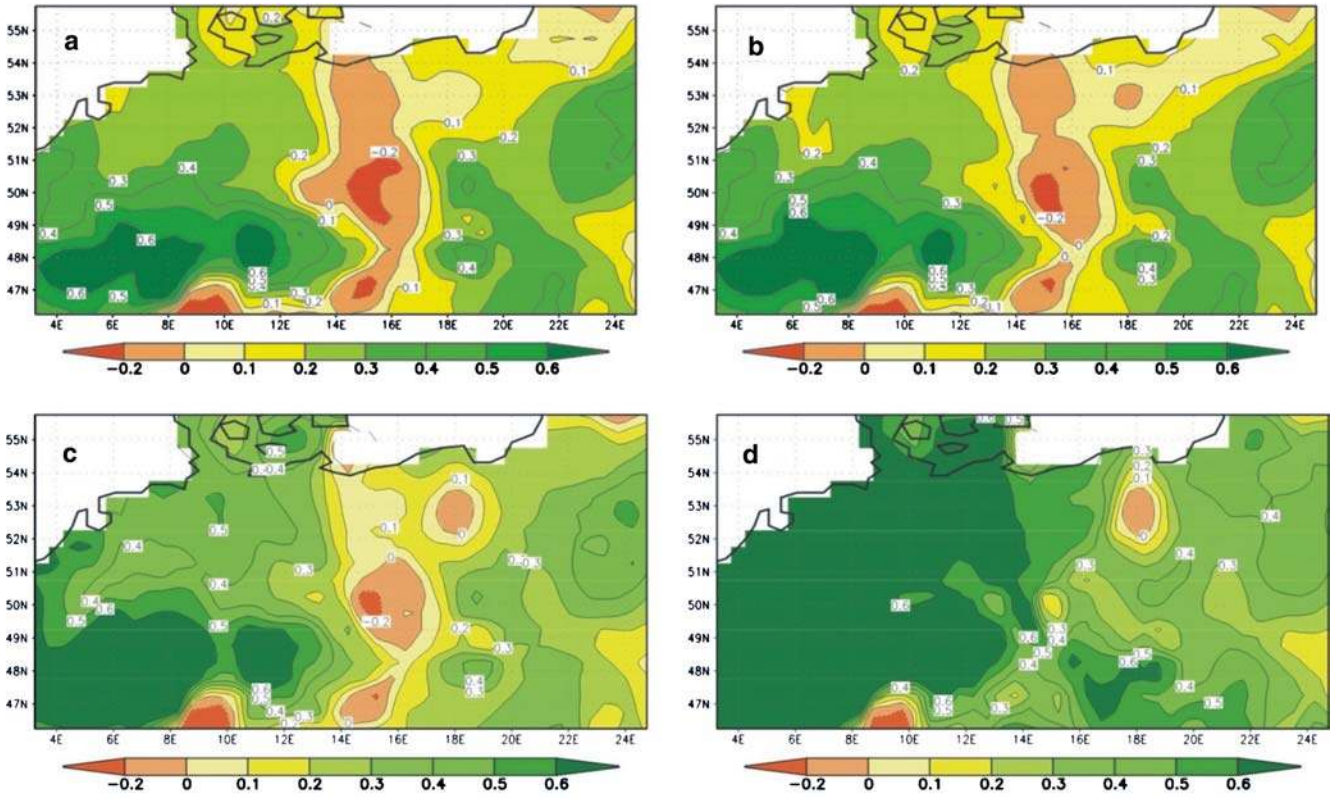

Fig. 4 As Fig. 3, but for the CEE reconstruction

RE values but the pattern is very similar to the one of winter.

3.3 Comparison with other reconstructions

For further validation of our reconstructions we compared them with a few selected regional precipitation reconstructions independent from ours. Wilson et al. (2005) reconstructed spring/summer precipitation based on tree-rings of the Bavarian Forest region. In Fig. 5a this series and the average of the corresponding nine grid points from the CEE reconstruction are displayed (also spring/summer mean). Correlations are highly significant for all centuries (Spearman's $rho_{critical,\ \alpha=5\%} = 0.19$, based on a two sided *t*-test). Although, there are no common predictors, the high correlation can at least partly be explained by the significant correlation of the chronology by Wilson et al. (2005) and the western Austrian network (Oberhuber and Kofler 2002; Strumia et al. 1997), which has been employed in our reconstruction. There is also less low-frequency variability in the Wilson et al. (2005) record than in our reconstruction. This may be due to the standardization of the tree-ring data in the Wilson et al. (2005) reconstruction. These results confirm that both reconstructions capture the same precipitation signal over the Bavarian Forest region.

Figure 5b shows the spring/summer precipitation reconstruction from the Czech Lands by Brázdil et al. (2002) together with the corresponding time series of our CEE reconstruction. The reconstructions are independent, i.e. they share no common predictors. The correlations are positive for all centuries although the two reconstructions do not agree in the low-frequency domain. This can be attributed at least partly to the standardization procedure of the tree-ring data and to the fact that tree-ring data often carry an annual temperature signal in their low-frequency domain (Frank and Esper 2005). The slightly lower correlation in the 19th century may be related to the low number of samples that are used in the development of this tree-ring chronology.

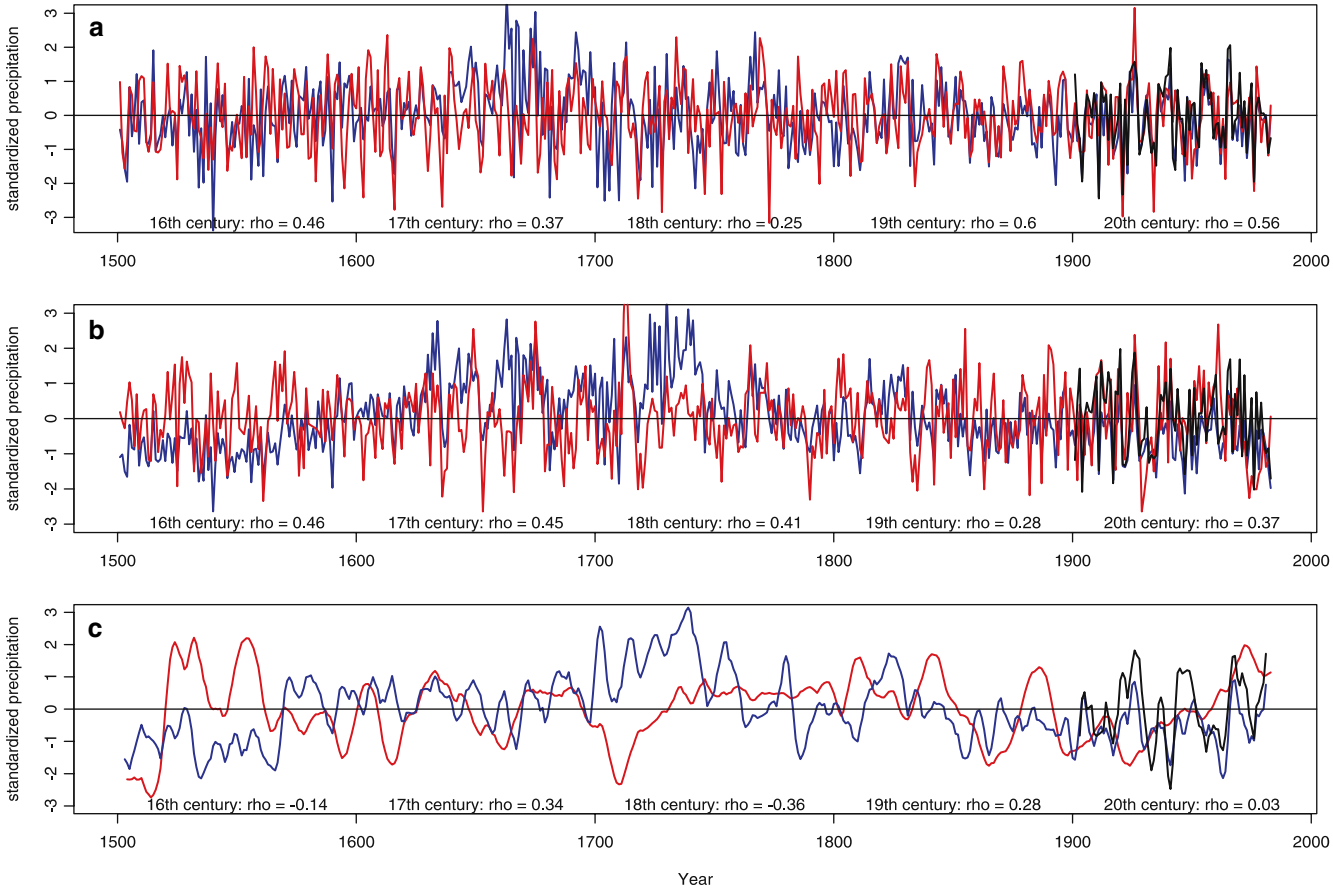

Fig. 5 Comparison of subregions of the CEE reconstruction with other independent reconstructions. Panel a: time series (spring/summer mean) of the reconstruction by Wilson et al. (2005; *red*) and the CEE reconstruction (*blue*) of the same region and season. Both time series are averages of the region 12.25–13.25°E/48.75–49.75°N. The black curve indicates the time series from the Mitchell and Jones (2005) data averaged over the same area. The indicated correlation coefficients are Spearman's rho and are calculated for one century. Panel b: as panel a, but for the Brázdil et al. (2002) reconstruction (Czech Lands). The area is given by 15.25–17.25°E/48.75–49.75°N. Panel c: as panel a, but for the Linderholm and Chen (2005) reconstruction (central Scandinavia). These curves are filtered using a 5-year-Gaussian filter. The time series are an average over the area 13–16°E/62–64°N

Brázdil et al. (2002) state that after 1956 correlations of their reconstruction with precipitation measurements drop to non-significant levels. So far, no satisfactory explanation can be given for this phenomenon (Brázdil et al. 2002) although it could be related to increased air pollution. Brázdil et al. (2002) further suggest that a combination of extremely dry years and air pollution (mainly NO_x, SO_2 and ozone) may disturb the climatic signal in tree-rings.

In a recent study, Linderholm and Chen (2005) reconstructed winter/spring precipitation in central Scandinavia using tree-ring data. Figure 5c depicts a comparison of this reconstruction with the spring series averaged over 13–16°E/62–64°N from our European reconstruction. In this area the chronologies used in the Linderholm and Chen (2005) study are located. Both series are filtered with a 5-year Gaussian filter. There is no significant overall correlation and the correlations change sign. Various reasons are possible for these conflicting results. A climate signal derived from tree-rings in that area is normally indicative of summer temperature (e.g. Briffa et al. 2001) and not precipitation. Additionally, according to Linderholm and Chen (2005) the strongest precipitation signal of tree-rings is September–April while we analyse March–May precipitation. We use only spring precipitation because reconstructive skill for winter in that region is very low. However, Linderholm and Chen (2005) find significant correlations with precipitation using 5-year averages and argue that tree-rings may contain information on winter precipitation variability via complex interactions between winter snow amount, ground frost and rain. Nonetheless, our reconstruction correlates highly significant ($r = 0.73$) with the Mitchell and Jones (2005) data for the same region and season while the Linderholm and Chen (2005) reconstruction and the Mitchell and Jones (2005) data disagree (Fig. 5c). It can be argued that this may be partly due to the fact that the climatic response in the tree-rings is best for September–April and not March–May. Still, during some periods the long-term fluctuations of the two curves is rather consistent.

3.4 Precipitation and large-scale circulation

3.4.1 Stability of the relation between precipitation and large-scale circulation

We restricted the running correlation analysis to winter, as during that season the dynamical relationship between precipitation and pressure is best pronounced in the northern extratropics. Figure 6a depicts 30-year running correlations of winter (DJF) precipitation averaged over Southern Spain and Morocco (10–0°W/33–40°N; see rectangles in Fig. 7) with the first three principal components (PC) of North Atlantic/European SLP reconstructions (see Fig. 7). We selected that region because its precipitation is known to be sensitive to the NAO (e.g. von Storch et al. 1993; Zorita et al. 1992; Hurrell and Loon 1997; Rodriguez-Puebla et al. 2001; Knippertz et al. 2003). These winter pressure reconstructions are based on temperature and pressure

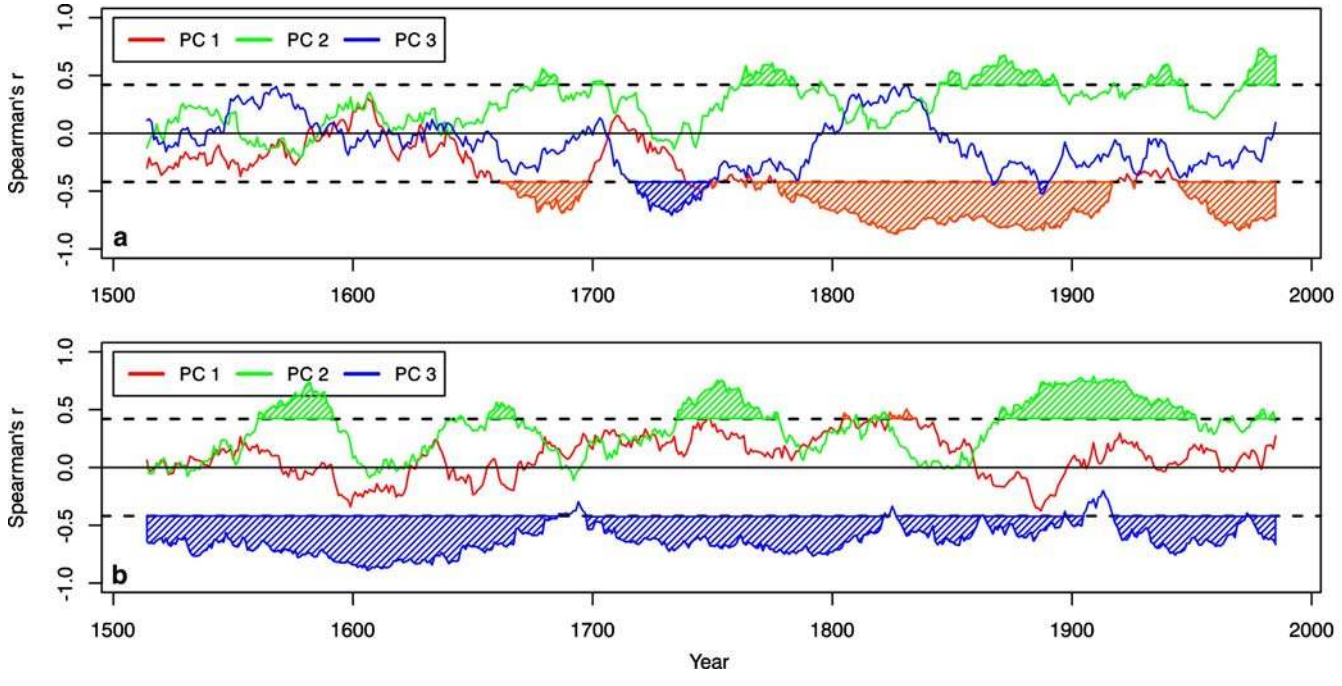

Fig. 6 Thirty-year running correlations of the first three principal components (PC) of winter (DJF) SLP reconstructions by Luterbacher et al. (2002a; calculated using no precipitation predictors) with winter (DJF) precipitation (**a**) averaged over Southern Spain and Morocco (see corresponding rectangle in Fig. 7) and (**b**) averaged over parts of central Europe (see corresponding rectangle in Fig. 7). The *dashed lines* denote the 5% significance threshold based on 1,000 Monte-Carlo simulations

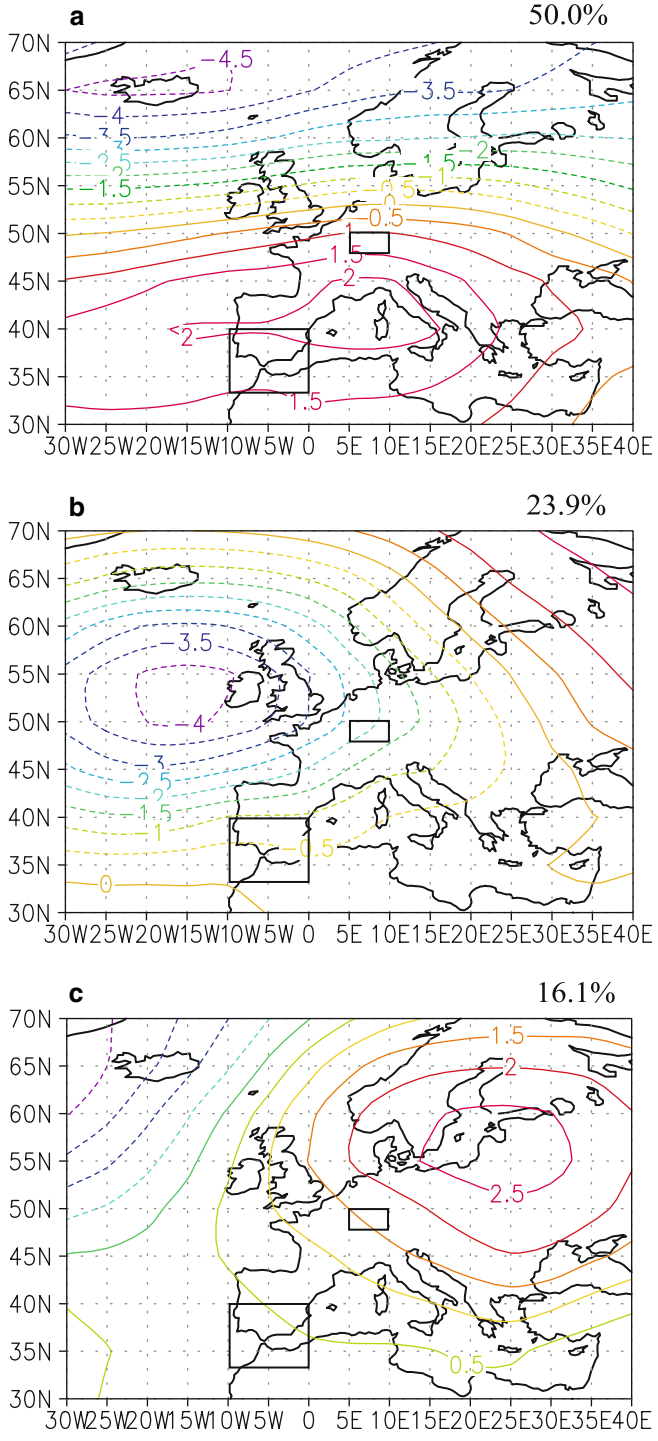

Fig. 7 First three EOFs of winter (DJF) SLP reconstructions 1500–2002 of the Luterbacher et al. (2002; version including no precipitation predictors). Contours represent normalized loadings. The percentages refer to the proportion of explained variance of each EOF

predictors (no precipitation predictors are included to ensure independence) and are described by Luterbacher et al. (2002a). Luterbacher et al. (2002a) noted that seasonal precipitation from Andalusia (Rodrigo et al. 1999, 2001) is a crucial predictor for skilful SLP reconstructions in southwestern Europe. Despite a few additional predictors, the exclusion of Andalusian precipitation in the independent reconstruction leads to lower skill, though still reliable SLP reconstructions within the 16th and 17th centuries.

EOF 1 (50.0% of explained variance, see Fig. 7a) is the most important pattern to explain winter precipitation variability over Southern Spain and Morocco during the late 17th century as well as during most of the 19th and 20th century. Correlations of the first PC with precipitation during these periods are negative and highly significant (see Fig. 6a). EOF 1 (Fig. 7a) is characterized by one centre over the western Mediterranean and the adjacent Atlantic and another centre over the North Atlantic around Iceland. This pattern resembles the NAO. Positive values of PC 1 are connected with a strong Azores high, covering Spain/Morocco. Westerlies are located further north. In its negative state (negative 'NAO') rather meridional circulation prevails which is connected with positive precipitation anomalies over southern Spain/Morocco.

Significant positive correlations of PC 2 (EOF 2 explains 23.9% of the total pressure variance, see Fig. 7b) with precipitation over Southern Spain and Morocco are found (see Fig. 6a). They occur periodically on quasi-centennial time scales. The spatial pattern of EOF 2 is featured by one centre of action west of Ireland. In its positive state the westerlies reach as far south as southern Spain/Morocco. They are connected with anomalous advection of moisture from the Atlantic Ocean to the European continent. Towards the end of the 17th, 18th, 19th and 20th century highly significant positive correlations occur while correlations occasionally drop to zero between these periods.

PC 3 (EOF 3 explains 16.1% of the SLP variance, see Fig. 7c) reveals highly significant negative correlations during the first half of the 18th century (see Fig. 6a). As seen from Fig. 7c, EOF 3 is associated with a 'blocking' pattern over the Baltic Sea and eastern Europe.

Interestingly, during the 18th century all three patterns sequentially dominate winter precipitation variability over Southern Spain and Morocco: EOF 1 is the most important pattern for precipitation variability at the end of the 18th century but correlations decrease to marginally significant values towards 1770. Meanwhile, correlations of PC 2 with precipitation increase. Around 1770, PC 2 is highly positively correlated with precipitation. Towards the first half of the 17th century, however, PC 3 played a key role in explaining precipitation variability over southern Spain and Morocco. Prior to 1650 most correlations are not significant, this might be partly be due to lower SLP reconstruction quality rather than a climatic signal.

Fig. 6b displays 30-year running correlations of winter (DJF) precipitation averaged over parts of central Europe (5–10°E/48–50°N; see rectangles in Fig. 7) and the time series of the three most important atmospheric patterns (Fig. 7). We chose that NAO-insensitive region

to contrast with the NAO-sensitive region of southern Spain/Morocco (e.g. Knippertz et al. 2003; Hurrell and Loon 1997; von Storch et al, 1993; Zorita et al. 1992). For this area, PC 3 is clearly correlated best with precipitation containing highly significant negative correlations over almost the whole period.

Similar to the correlations in Fig. 6a, PC 2 is positively correlated during the late 16th century, around 1650 and 1750 and during the period 1850–1950.

PC 1 is rarely significantly correlated with precipitation averaged over this study area and correlation sign changes frequently over the last 500 years. This suggests that it is of minor importance for precipitation variability over central Europe.

To sum up, correlations of the PCs with precipitation over southern Spain/Morocco and central Europe vary during the last 500 years on decadal timescales. PC 1 is the most important pattern for precipitation over southern Spain/Morocco. PC 2 is only relevant during some periods. Interestingly, PC 3 was important during the first part of the 18th century. Regarding central Europe PC 3 dominates precipitation throughout the last 500 years. The two other patterns are less important. However, PC 2 also correlates highly significantly with central European precipitation during several periods.

3.4.2 *Relationship of precipitation extremes and large-scale circulation*

To investigate the relationship between winter precipitation extremes (here defined as the 5% wettest or driest winters of the 1500–2000 period) and atmospheric circulation we calculated scaled composites (cf. Sect. 2.3.4) and the associated SLP anomaly patterns. Figure 8 displays scaled composite anomaly maps with corresponding pressure anomalies for the 5% wettest (Fig. 8a, b) and driest winters (Fig. 8c, d) over southern Spain/northern Morocco (region is marked by black rectangles in Fig. 8) over the last 500 years. Hence, both scaled anomaly maps are based on 25 winters. The wet pattern (Fig. 8a) reveals significant negative precipitation anomalies over large parts of the Mediterranean basin, while significant positive anomalies occur over Scotland, Ireland, Norway and over the region extending from northern France to Finland. The associated independent pressure anomaly pattern (Fig. 8b) shows a

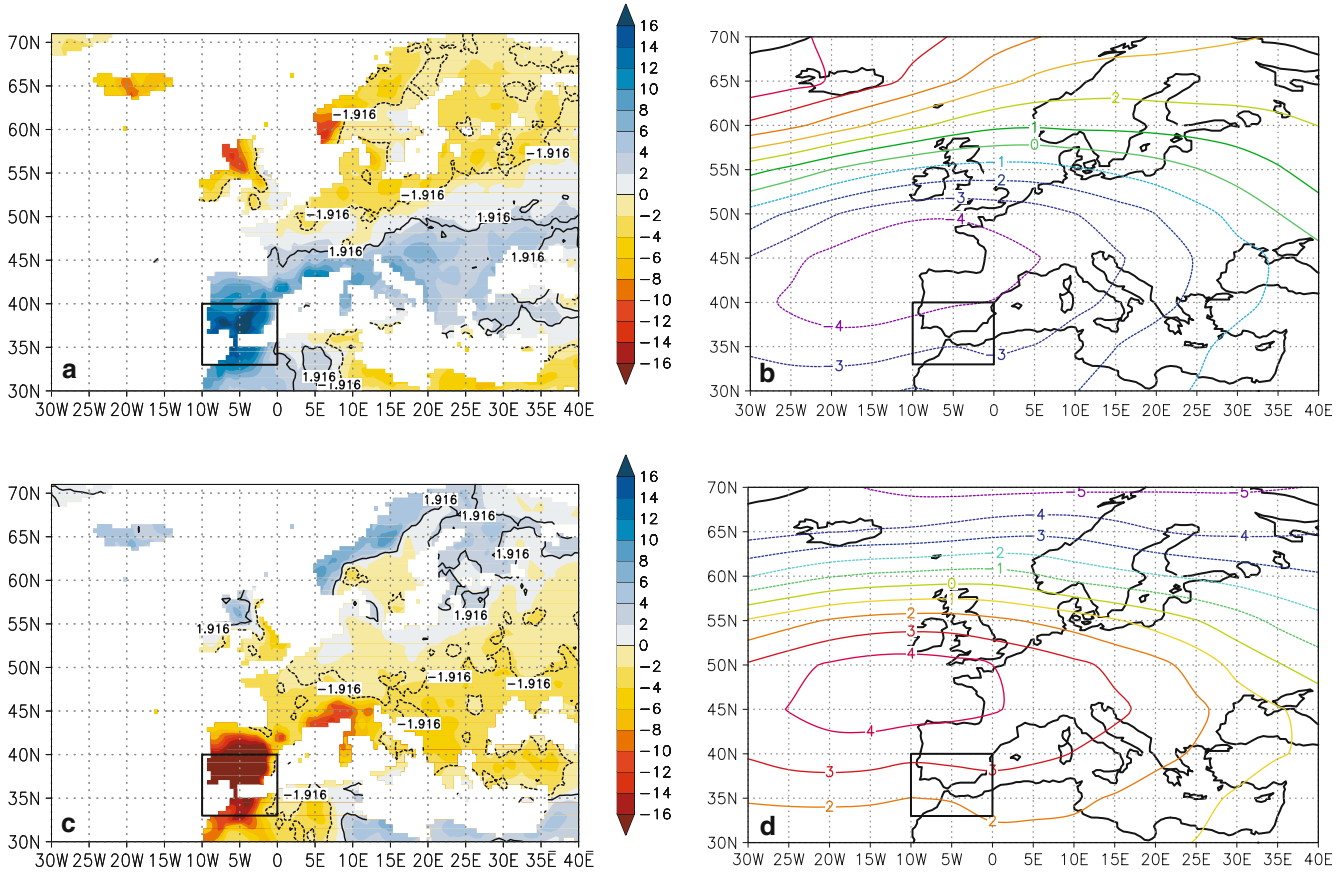

Fig. 8 Scaled anomaly composites of winter (DJF) precipitation (**a**, **c**) and corresponding pressure anomalies (**b**, **d**; in hPa; relative to 1901–2000). The composite precipitation maps are based on the 5% wettest (panel a) and driest winters (panel c) over southern Spain/northern Morocco (*black rectangle*) of the period 1500–2000. Units are dimensionless. The significance thresholds (±1.916) are based on a modified *t*-test (Brown and Hall 1999)

dominating negative centre over northern Spain and the adjacent Atlantic Ocean while positive pressure anomalies occur over Iceland.

Figure 8c shows the composite for the 5% driest winters. It is largely the opposite of the pattern in Fig. 8a: significant dry anomalies occur over the northern parts of the Mediterranean basin, while Scotland and large parts of Scandinavia experience wet conditions. Over parts of central Europe no significant anomalies can be observed. The associated pressure anomalies (Fig. 8d) features largely the opposite pattern of the wet anomalies with a positive centre over western France and the adjacent Atlantic Ocean.

Figure 9a depicts scaled composite maps based on the 5% wettest (driest) winters over central Europe (black rectangle) over the period 1500–2000. Again, each map is based on 25 winters. Almost all areas show significant anomalies: while over Europe (excluding western Scandinavia) very wet conditions prevail, significant dry anomalies can be observed over north Africa, Iceland and Norway. The associated anomaly pressure pattern (Fig. 9b) is characterized by negative SLP anomalies over the North Sea and positive SLP departures over Iceland/Greenland.

In the case of very dry conditions over central Europe (Fig. 9c) the opposite pattern dominates: Significant dry conditions over most parts of Europe and significant positive anomalies over Greenland/Iceland, Norway and north Africa including southern parts of the western Mediterranean. The corresponding SLP pattern (Fig. 9d) depicts a strong positive anomaly over the British Isles. A negative centre is located west of the North African coast.

To sum up, winter precipitation anomalies over southern Spain/Morocco are associated with pressure anomalies centred over the Atlantic Ocean northwest of the Iberian Peninsula. Further, these anomalies coincide with anomalies over most parts of the Mediterranean, Scotland and Scandinavia. Central European winter precipitation extremes are connected with pressure over the North Sea and the British Isles. They also show significant connections to precipitation over Scandinavia and the Mediterranean.

4 Discussion

4.1 Reconstructive skill

The reconstructive skill for gridded precipitation of the 17th century remains at the same level as during the 16th century in most regions but increases substantially dur-

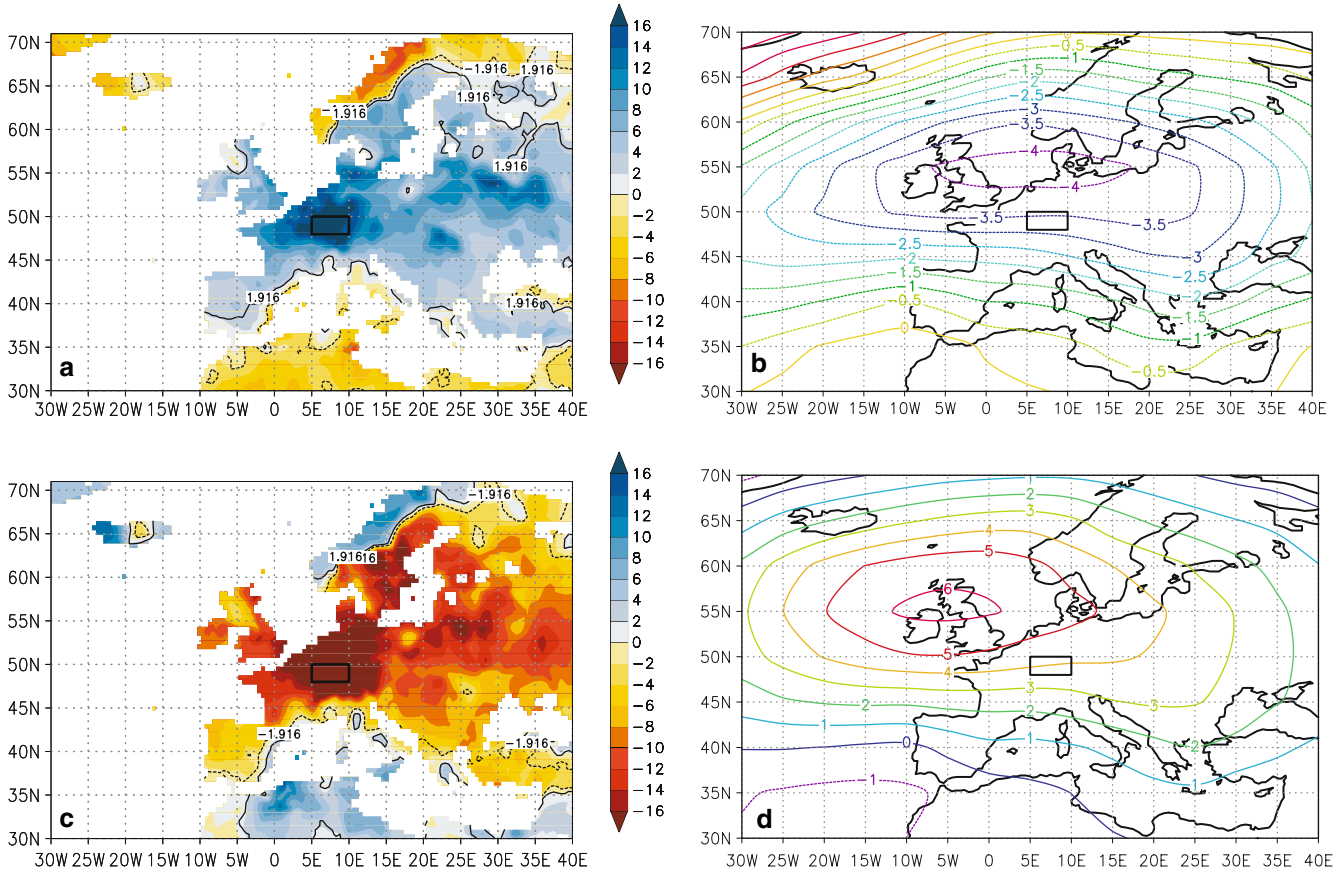

Fig. 9 As Fig. 8, but for central Europe

ing the 18th and 19th century for the European reconstructions (Fig. 3). A reason for this is the number, type, quality and the location of predictors that have become available towards the present time. The long instrumental series start during the 18th century when also more tree-ring chronologies become available (the list of predictors can be found in the electronic supplementary material). Additionally, documentary precipitation indices are not available continuously throughout the whole reconstruction period back to 1500. An example is the sharp increase in 1675 and decrease in 1715 of the RE values over southern Spain/Morocco (not shown). This fluctuation coincides with the availability of documentary indices from several Spanish cities during that period (Martin-Vide and Barriendos 1995; Barriendos 1997, 2005; Rodrigo et al. 1999, 2001).

The regions with high reconstructive skill are also linked to the location of the proxies. In central Europe documentary indices are available (Pfister 1999; Rácz 1999), whereas in eastern Europe precipitation-sensitive tree-rings exist and for Spain and Morocco both tree-rings and documentary indices can be found. Given the high spatial variability of precipitation it is not surprising that reconstructive skill varies substantially in space. Hence, it is difficult to skilfully reconstruct precipitation in areas where no predictor information is available due to a lack of precipitation signals of remote regions for such regions. For instance, there are no long predictors in Italy, which may be the reason for the poor reconstructive skill over that region (see Fig. 3). This highlights the need for well-distributed predictors resolving the precipitation signal at seasonal scale (e.g. Luterbacher et al. 2005).

The three regional reconstructions reveal slightly higher RE values than the corresponding REs of the European reconstruction (see Fig. 4 and the electronic supplementary material). This shows that by calibrating regional predictors against a regional field there is a potential for improving the reconstructions. However, this is only feasible if suitable predictors are available in the region, and in many cases it has been proven to be impossible to rely on teleconnections. Luterbacher et al. (2002a, 2004) reported skilful SLP and temperature reconstructions for Europe using remote predictors. However, this study suggests that local predictors are essential in many cases with precipitation as the target variable. An exception may be southern Spain where the European reconstruction (Fig. 3) reveales higher RE values than the IPM reconstruction (see the electronic supplementary material) that was produced using exclusively local predictors. This can be explained with the high precipitation sensitivity of that region to the NAO. Proxies that record NAO variability but are remote to southern Spain can still be meaningful for precipitation reconstructions in that area. Hence, in this case it is recommended not only to use local predictors due to possible teleconnections.

As seen in Fig. 4, the RE values over Poland and the eastern part of Germany are below zero for all centuries although there are tree-ring predictors available and documentary indices are located in Germany and the Czech Lands. This may be related to features in the Mitchell and Jones (2005) dataset. New et al. (2000) report that there may be inhomogeneities in the station observations that were used to develop the Mitchell and Jones (2005) dataset. Further, before World War II the Mitchell and Jones (2005) dataset relies on only two station observations for the whole of Poland (New et al. 2000). According to Dai et al. (1997) two annual precipitation stations have only 50% of the variance in common when located 80 km apart. During summer this distance is smaller given the mainly convective nature of precipitation. Especially in summer there are grid points over Poland with very low RE values in the CEE reconstruction (not shown). Hence, new stations in a region the size of Poland can substantially alter grid point values of the Mitchell and Jones (2005) dataset. This may lead to underestimated RE values as the model is fitted to a predictand field that was developed using only two stations for the whole Poland (1901–1956). When verification was performed during 1957–1983 many more stations were used to produce the predictand field leading to different characteristics of the predictand. As the final models for the reconstruction are calculated using the whole period 1901–1983 the quality of the reconstructions may be higher than estimated by the RE values. Supporting evidence of this interpretation are the very low RE values in summer (< -0.2) as the spatial precipitation variability is highest in this season over this region.

Similar reasons could be important for the poor reconstructive skill over Turkey, southern Italy and southern France (see Fig. 3). In Turkey, for example, there are only very few coastal station observations available from the 1930s onward and none in the interior of this country (New et al. 2000; Mitchell and Jones 2005; Turkes 1996, 1998; Turkes and Erlat 2003; Touchan et al. 2005; Xoplaki et al. 2004). A collection of starting dates of Mediterranean precipitation measurements can be found in Xoplaki et al. (2004).

The performance of the reconstruction over some parts of the European Alps is also reduced. At 9°E/46°N, RE values are negative (Figs. 3, 4). One may argue that this is an area located on the south side of, or within the Alpine mountain range, which thus has different precipitation characteristics than the northern side of the Alps where the predictors are located. From within the Alpine mountain range no predictors could be used. Hence, well-distributed and dense predictor coverage as well as observation stations are particularly important in mountainous regions with a complex terrain and different precipitation regimes. However, the neighbouring region of the Valais shows high reconstructive skill ($RE > 0.4$, see Fig. 4). This may be attributed to the relative dryness and low variability of that region. Frei und Schär (1998) argue that the Valais is subject to "inner-alpine shielding" which makes its precipitation characteristics rather continental. Further possible reasons for the high reconstructive skill include

the proximity of the Valais to the northern side of the Alps whereas the Alpine range becomes much wider towards the east.

Interestingly, there are very low RE values for the region of the Czech Republic although a documentary index is available for that area (see Fig. 4). The reason for this apparent contradiction could be the discontinuous documentary record. Two thirds of the 16th century values are missing and for the 17th and 18th century no values are available at all. This contrasts with the area of Hungary where a continuous documentary record could be used. Over that area RE values range from 0.1 to over 0.4 throughout the whole reconstruction period.

4.2 Precipitation and large-scale circulation

The varying correlations of the major atmospheric patterns and precipitation over southern Spain and Morocco as well as over central Europe indicate non-stationarities in the European/North Atlantic climate system (Fig. 6). Touchan et al. (2005) found non-stationary and insignificant relationships between major European-scale circulation patterns and eastern Mediterranean late spring/summer precipitation over the last 237 years. Further, Jacobeit et al. (2003) report that the long-term evolution of increasing anticyclonicity over Europe during July has strengthened during the last 50 years, becoming recently a unique phenomenon within the last centuries and causing an unprecedented decline in central European July precipitation during the second half of the 20th century. Casty et al. (2005b) report on non-stationary behaviour of climate regimes over the North Atlantic/European region in reconstructed and modelled SLP data back to 1659. Hence, these studies found major instationarities in European climate as well.

Winter precipitation over southern Spain and Morocco is believed to be mainly determined by the state of the NAO (e.g. Knippertz et al. 2003; von Storch et al. 1993; Rodriguez-Puebla et al. 2001; Zorita et al. 1992), whose spatial pattern is well represented by EOF 1 displayed in Fig. 7a. During the second part of the 17th century, PC 1 is most significantly correlated with precipitation although PC 2 is important too (Fig. 6a). This period of the Maunder Minimum seemed to be controlled by the NAO, which often remained in its negative state (Luterbacher et al. 1999, 2001, 2002b).

However, our results show that the connection of precipitation to large-scale atmospheric circulation is not stable over time at decadal timescales and suggest that different patterns (not only the NAO) have played a role in determining precipitation variability over southern Spain and Morocco (Fig. 6a). This is also true for the period around 1930 when correlations drop to partly insignificant levels. Interestingly, PC 2 correlates significantly with precipitation during that period which suggests that EOF 2 (Fig. 7b) was equally important to the NAO-pattern (Fig. 7a) in terms of explaining winter precipitation variability over southern Spain and Morocco.

EOF 3, a continental 'blocking', and its corresponding PC time series influenced large parts of central European climate during the Maunder Minimum (1645–1715; Luterbacher et al. 2001). The significant correlations of PC 3 with precipitation during the first half of the 18th century suggest that the influence of EOF 3 reached as far southwest as southern Spain and Morocco.

The pre-1650 period is characterized by overall low correlations (Fig. 6a). From a dynamical perspective this is rather surprising, as winter precipitation has to be linked to large-scale circulation. However, this feature may be associated with decreasing reconstructive skill of both the SLP and the precipitation reconstructions. In the European reconstruction, the network of documentary indices becomes much denser over Spain, Portugal and Greece from 1675 to 1715 (Alcoforado et al. 2000; Barriendos 1997; Martin-Vide and Barriendos 1995; Rodrigo et al. 1999, 2001; Xoplaki et al. 2001). Nevertheless, even the 16th century reconstructive skill was estimated to be high over southern Spain and Morocco (see Fig. 3). Concerning the SLP reconstructions, the longest pressure series used by Luterbacher et al. (2002a) starts in 1670 (Paris; Slonosky et al. 2001a). That time approximately coincides with the drop of the correlations. The sharp decrease of the correlation between the PC 1 of SLP and winter precipitation during the early 18th century may also be partially related to predictor availability as data of the Paris pressure series is missing during July 1713 to December 1763. The same is reported for the London series, which starts in 1697 (Slonosky et al. 2001a). For this series the gap includes the years 1709–1773. However, new pressure series become available from Uppsala (1722) and Basel (1744). Hence, between 1713 and 1722 the pressure reconstructions are based solely on temperature information. To summarize, the changes of the correlation coefficients up to around 1750 may at least partly be related to predictor availability.

Figure 6b depicts the running correlations of winter precipitation averaged over parts of central Europe and the time series of the three most important patterns (Fig. 7a–c). Correlation of central European precipitation with the time series of PC 1 (or the NAO) is not continuously significant for the last 500 years (Fig. 6b). This agrees with findings by Hurrell and Loon (1997) who found central European winter precipitation to be rather insensitive to changes of the NAO during 1900–1994. Our results suggest that this is true for the past 500 years. Casty et al. (2005a) calculated 31-year running correlations of Alpine precipitation (December–March) with the NAO back to 1659. They found significant negative correlations during the periods 1860–1920 and after 1950. However, before those periods, correlations are hardly significant, which agrees with our results. At the end of the 19th century, our correlations (Fig. 6b) also show negative correlations, though hardly signifi-

cant. We attribute the different results to the different areas that were analysed. We used a region further north to the Alps (cf. Fig. 7) while Casty et al. (2005a) investigated the Alpine area including the south side of the Alps where precipitation contains a Mediterranean signal of the NAO (Hurrell and Loon 1997).

The correlation of the time series of EOF 2 with winter precipitation over central Europe (Fig. 6b) fluctuates on multi-decadal timescales with highly significant correlations around 1900, 1750 and 1650, and during the second half of the 16th century. As seen from Fig. 7b the main pressure centre of the associated pattern is located west of Ireland. In case of high pressure the westerlies are blocked and northerly relatively dry winds prevail. In case of low pressure, mild air is advected from the Atlantic and brings moisture to central Europe.

Over the whole 500 years, the PC 3 is correlated best with precipitation. Significant negative correlations are found over almost the whole period. This corroborates the validity of both the SLP and the precipitation reconstructions over Europe back to 1500. A pressure centre over northeastern Europe characterizes the associated EOF 3 pattern (Fig. 7c). In the case of positive SLP anomaly, dry and cold conditions prevail over central Europe. The negative state is associated with wet conditions in the northern Alps. These situations are known to be responsible for heavy winter snowfall over that region resulting in positive glacier mass balance (Wanner et al. 2000).

4.3 Relationship of precipitation extremes and large-scale circulation

The scaled winter anomaly composites presented in Fig. 8a, c show a typical NAO pattern (e.g. Hurrell and Loon 1997; Wanner et al. 2001): wet (dry) conditions over southwestern Europe coincide with dry (wet) periods over northern Europe. Between these regions possible anomalies cancelled while producing the composite. The distinct patterns with highly significant anomalies suggest that this precipitation distribution during extreme winters re-occurred during the last 500 years. The negative pressure anomaly over northern Spain and the adjacent Atlantic Ocean (Fig. 8b) facilitates advection of moist air from the Atlantic and the overall influence of the low triggers precipitation over southern Spain and Morocco. This is in line with the reconstructed wet anomalies (Fig. 8a). In case of dry periods (Fig. 8c), southern Spain and Morocco are dominated by high pressure, which suppresses precipitation. Anomalous easterly winds over southern Europe prevent moist oceanic air from reaching southern Spain and Morocco. Provided this pressure distribution, that region is uncoupled from the westerlies that are located further north and cause northern Europe to experience very wet conditions.

Taking into account the anomaly patterns from central Europe (Fig. 9a, b) it can be argued that low pressure over the North Sea triggers precipitation over central and eastern Europe. The Mediterranean and northern Africa are relatively dry as lows infrequently reach that region. The Scandinavian mountain range experiences dry anomalies as well. This may be due to weakened westerlies or even prevailing easterly winds. East of the Scandinavian mountains these winds along with general low pressure influence, cause wet conditions.

In case of dry anomalies over central Europe (Fig. 9c, d) the opposite pattern dominates. High pressure over the British Isles brings moist oceanic air to the Scandinavian mountain range while the remaining part of Scandinavia is left dry. High pressure also impedes precipitation over central and eastern Europe as well as large parts of Spain and Turkey. Only parts of the Mediterranean and North Africa have wetter conditions than normal, which may be explained by low pressure influence.

5 Conclusions and outlook

We present seasonally resolved gridded precipitation reconstructions over the last 500 years for the European region. This kind of dataset was hitherto not available. It was developed using PCR techniques. Despite discussed constraints (e.g. predictor availability and regional precipitation regimes) these precipitation reconstructions provide a very useful basis on which past precipitation variability can be analysed. They agree well with independent reconstructions for selected areas. Winter precipitation reconstructions showed highest reconstructive skill compared to the other seasons. Moreover, the quality of the reconstructions decreases back in time. Still, various regions showed high reconstructive skill back to 1500.

We demonstrated that there are major instationarities in the relationship between precipitation over southern Spain/Morocco and the three most important patterns of atmospheric circulation. During the last 500 years different patterns have been important to explain precipitation variability. The same conclusion can be drawn for central Europe.

Using scaled composite analysis we showed that winter precipitation extremes over southern Spain/northern Morocco are connected to atmospheric pressure anomalies over the Atlantic northwest of the Iberian Peninsula and support recent findings, though for a longer time period. For central European precipitation anomalies, SLP over the North Sea and the British Isles are important. Joint analysis of precipitation extremes of the last 500 years over these regions and pressure anomalies revealed consistent patterns that can be synoptically well interpreted. This further supports the validity of the precipitation reconstructions.

For the first time it is possible to perform detailed precipitation studies on a regional and continental scale. Apart from the presented analyses of the precipitation/pressure stability, subsequent studies could involve tem-

perature as well (Casty et al. 2005c). Further applications of this new dataset include investigations of the causes of historic glacier fluctuations. Using this dataset, Steiner et al. (2005) reported that several combinations of seasonal temperature and precipitation led to the advances and retreats of European glaciers during the 'Little Ice Age'. Raible et al. (2005) compared both these reconstructions and temperature with model simulations. Such analyses can help improve our understanding of natural and anthropogenic climate variability. Moreover, as reconstructions are available for all seasons, studies will now be possible dealing with seasonal climate change such as seasonal shifts.

Acknowledgements This work is part of the EU-project SOAP: simulations, observations and palaeoclimate (data: climate variability over the last 500 years) the Swiss part being funded by the Staatssekretariat für Bildung und Forschung (SBF) under contract 01.0560. Publication of this work was also supported by the Marchese Francesco Medici del Vascello foundation. Jürg Luterbacher is supported by the Swiss National Science foundation through its National Center of Competence in Research in Climate program, project PALVAREX. Carlo Casty is funded by the European Commission under the Fifth Framework Programme Contract Nr. EVR1-2002-000413, project PACLIVA. The predictand data has been kindly provided by the Climatic Research Unit in Norwich, United Kingdom, and by the Tyndall Centre for Climate Change Research. The authors also wish to thank two anonymous reviewers for their helpful comments, Anita Orme for English corrections and the following persons for access to their data: Rudolf Brázdil, Michael Grabner, Hans Linderholm, Walter Oberhuber, Rob Wilson (all tree-ring data), Mariano Barriendos, Rudolf Brázdil, Rüdiger Glaser, Christian Pfister, Lajos Rácz, Fernando Rodrigo, Elena Xoplaki (all documentary data) and also many data contributors to the World Data Center for Paleoclimatology, Boulder, Colorado, USA.

References

Akkemik Ü, Aras A (2005) Reconstruction (1689–1994 AD) of April–August precipitation in the southern part of central Turkey. Int J Climatol 25:537–548, DOI 10.1002/joc.1145

Akkemik Ü, Dağdeviren N, Aras A (2005) A preliminary reconstruction (A.D. 1635–2000) of spring precipitation using oak tree-rings in the western Black Sea region of Turkey. Int J Biometeorol 49:297–302, DOI 10.1007/s00484-004-0249-8

Alcoforado MJ, Nuñes MF, Garcia JC, Taborda JP (2000) Temperature and precipitation reconstructions in southern Portugal during the Late Maunder Minimum (1675–1715). Holocene 10:333–340

Barriendos M (1997) Climatic variations in the Iberian Peninsula during the late Maunder Minimum (AD 1675–1715): an analysis of data from rogation ceremonies. Holocene 7:105–111

Barriendos M (2005) Climate and culture in Spain, religious responses to extreme climatic events in the Hispanic Kingdoms (16th to 19th centuries) In: Behringer W, Lehmann H, Pfister C (eds) Cultural consequences of the 'Little Ice Age' ('Kulturelle Konsequenzen der Kleinen Eiszeit'). Vandenhoech and Ruprecht, Göttingen, pp 31–86

Barriendos M, Rodrigo FS (2005) Seasonal rainfall variability in the Iberian Peninsula from the 16th century: preliminary results from historical documentary sources, Geophys Res Abstracts 7

Brázdil R, Friedmannová L (1994) Temperature patterns in the Czech Lands in 1751–1850—comparison of documentary evidence and of instrumental data. In: Brázdil R, Kolár M (eds) Contemporary climatology. Proceedings of the meeting of the commission on climatology of the international geographical union, 15–20 August 1994, Brno, Czech Republic, pp 82–92

Brázdil R, Pfister C, Wanner H, von Storch H, Luterbacher J (2005) Historical climatology in Europe—the state of the art. Clim Change 70:363–430

Brázdil R, Stepanková P, Kyncl T, Kyncl J (2002) Fir tree-ring reconstruction of March–July precipitation in southern Moravia (Czech Republic), 1376–1996. Clim Res 20:223–239

Brázdil R, Valášek H, Macková J (2003) Climate in the Czech Lands during the 1780s in the light of daily weather records of Parson Karel Bernard Hein of Hodonice (south-western Moravia): comparison of documentary and instrumental data. Clim Change 60:297–327

Briffa KR, Osborn TJ, Schweingruber FH, Harris IC, Jones PD, Shiyatov SG, Vaganov EA (2001) Low-frequency temperature variations from a northern tree ring density network. J Geophys Res 106:2929–2941

Briffa KR, Osborn TJ, Schweingruber FH, Jones PD, Shiyatov SG, Vaganov EA (2002) Tree-ring width and density data around the northern hemisphere: part 1, local and regional climate signals. Holocene 12:737–757

Brönnimann S, Luterbacher J (2004) Reconstructing Northern Hemisphere upper-level fields during World War II. Clim Dynam 22:499–510, DOI 10.1007/s00382-004-0391-3

Brown TJ, Hall BL (1999) The use of t values in climatological composite analyses. J Clim 12:2941–2945

Camuffo D (1984) Analysis of the series of precipitation at Padova, Italy. Clim Change 6:57–77

Casty C, Wanner H, Luterbacher J, Esper J, Böhm R (2005a) Temperature and precipitation variability in the European Alps since 1500. Int J Climatol 25:1855–1880 DOI 10.1002/joc1216

Casty C, Handorf D, Raible CC, Gonzalez-Rouco JF, Weisheimer A, Xopaki E, Luterbacher J, Dethloff K, Wanner H (2005b) Recurrent climate winter regimes in reconstructed and modelled 500 hPa geopotential height fields over the North Atlantic/European sector 1659–1990. Clim Dynam 24:809–822

Casty C, Handorf D, Sempf M (2005c) Combined climate winter regimes over the North Atlantic/European sector 1766–2000. Geophys Res Lett 32, L13801, DOI 10.1029/2005GL022431

Cook ER, Briffa KR, Jones PD (1994) Spatial regression methods in dendroclimatology—a review and comparison of two techniques. Int J Climatol 14:379–402

Cook ER, Holmes RL (1986) Users manual for program ARSTAN. Laboratory of Tree-Ring Research, University of Arizona, Tucson, USA

Cook ER, Woodhouse CA, Eakin CM, Meko DM, Stahle DW (2004) Long-term aridity changes in the western United States. Science 306:1015–1018, DOI 10.1126/science.1102586

Dai A, Fung IY, Del Genio AD (1997) Surface observed global land precipitation variations during 1900–1988. J Clim 10:2943–2962

D'Arrigo RD, Cullen HM (2001) A 350-year (AD 1628–1980) reconstruction of Turkish precipitation. Dendrochronologia 19:167–177

Diodato N (2006) A 425-year precipitation history from documentary weather anomalies and climate records at Palermo: Astronomical Observatory (Sicily, Italy). PAGES News, 14/1 (in press)

Felis T, Pätzold J, Loya Y, Fine M, Nawar A, Wefer G (2000) A coral oxygen isotope record from the northern Red Sea documenting NAO, ENSO, and North Pacific teleconnections on Middle East climate variability since the year 1750. Paleoceanography 15:679–694

Folland CK, Rayner NA, Brown SJ, Smith M, Shen SSP, Parker DE, Macadam I, Jones PD, Jones RN, Nicholls N, Sexton DMH (2001) Global temperature change and its uncertainties since 1861. Geophys Res Lett 28:2621–2624

Frank D, Esper J (2005) Temperature reconstructions and comparisons with instrumental data from a tree-ring network for the European Alps. Int J Climatol 25:1437–1454

Frei C, Schär C (1998) A precipitation climatology of the Alps from high-resolution rain-gauge observations. Int J Climatol 18:873–900

García-Herrera R, Macías A, Gallego D, Hernández E, Gimeno L, Ribera P (2003) Reconstruction of the precipitation in the Canary Islands for the period 1595–1836. B Am Meteorol Soc 84:1037–1039

Gershunov A, Schneider N, Barnett T (2001) Low-frequency modulation of the ENSO—Indian monsoon rainfall relationship: signal or noise? J Clim 14:2486–2492

Gimmi U, Luterbacher J, Pfister C, Wanner H (2005) A method to reconstruct long precipitation series using systematic descriptive observations in weather diaries: the example of the precipitation series for Bern, Switzerland (1760–2003). Theor Appl Climatol (in press)

Glaser R (2001) Klimageschichte Mitteleuropas: 1000 Jahre Wetter Klima, Katastrophen. Primus Verlag, Darmstadt, p 227

Hirschboeck KK (1988) Flood hydroclimatology. In: Baker VR, Kochel RC, Patton PC (eds) Flood geomorphology. Wiley, New York, pp 27–49

Hurrell JW, van Loon H (1997) Decadal variations in climate associated with the North Atlantic Oscillation. Clim Change 36:301–326

International Tree-Ring Data Bank (ITRDB) (2005) Data Bank maintained by the NOAA Paleoclimatology Program and the World Data Center Paleoclimatology http://www.ncdc.noaa.gov/paleo/treering.html

IPCC (2001) Climate Change 2001: the scientific basis. Contribution of working group I to the third assessment report of the Intergovernmental Panel on Climate Change. Cambridge University Press, Cambridge, UK and New York, USA

Jacobeit J, Glaser R, Luterbacher J, Wanner H (2003) Links between flood events in Central Europe since AD 1500 and large-scale atmospheric circulation modes. Geophys Res Lett 30:1172–1175, DOI 10.1029/2002GL016433

Jacobeit J, Jönsson R, Bärring L, Beck C, Ekström M (2001) Zonal indices for Europe 1780–1995 and running correlations with temperature. Clim Change 48:219–241

Jones PD, Mann ME (2004) Climate over past millennia. Rev Geophys 42 RG2002, DOI 10.1029/2003RG000143

Jones PD, Osborn TJ, Briffa KR (2003) Pressure-based measures of the North Atlantic Oscillation (NAO): a comparison and an assessment of changes in the strength of the NAO and in its influence on surface climate parameters. In: Hurrell JW, Kushnir Y, Ottersen G, Visbeck M (eds) The North Atlantic Oscillation: climatic significance and environmental impact. Geophysical monograph, vol 134, American Geophysical Union, Washington

Knippertz P, Christoph M, Speth P (2003) Long-term precipitation variability in Morocco and the link to the large-scale circulation in recent and future climates. Meteorol Atmos Phys 83:67–88

Linderholm HW, Chen D (2005) Central Scandinavian winter precipitation variability during the last five centuries reconstructed from Pinus sylvestris tree rings. Boreas 34:43–52

Luterbacher J et al (2005) Mediterranean climate variability over the last centuries; a review. In: Lionello P, Malanotte-Rizzoli P, Boscolo R (eds) The Mediterranean climate: an overview of the main characteristics and issues. Elsevier (in press)

Luterbacher J, Dietrich D, Xoplaki E, Grosjean M, Wanner H (2004) European seasonal and annual temperature variability, trends and extremes since 1500. Science 303:1499–1503

Luterbacher J, Rickli R, Xoplaki E, Tinguely C, Beck C, Pfister C, Wanner H (2001) The late maunder minimum (1675–1715)—a key period for studying decadal scale climatic change in Europe. Clim Change 49:441–462

Luterbacher J, Schmutz C, Gyalistras D, Xoplaki E, Wanner H (1999) Reconstruction of monthly NAO and EU indices back to AD 1675. Geophys Res Lett 26:2745–2748

Luterbacher J, Xoplaki E, Dietrich D, Rickli R, Jacobeit J, Beck Z, Gyalistras D, Schmutz C, Wanner H (2002a) Reconstruction of sea-level pressure fields over the eastern North Atlantic and Europe back to 1500. Clim Dynam 18:545–561

Luterbacher J, Xoplaki E, Dietrich D, Jones PD, Davies TD, Portis D, Gonzalez-Rouco JF, von Storch H, Gyalistras D, Casty C, Wanner H (2002b) Extending North Atlantic Oscillation reconstructions back to 1500. Atmos Sci Lett 2:114–124, DOI 10.1006/ asle.2001.0044

Mann ME, Rutherford S (2002) Climate reconstruction using 'pseudoproxies'. Geophys Res Lett 29:1501–1504, DOI 10.1029/2001GL014554

Mann ME, Rutherford S, Wahl E, Ammann C (2005) Testing the fidelity of methods used in proxy-based reconstructions of past climate. J Clim 18:4097–4107

Martin-Vide J, Barriendos M (1995) The use of rogation ceremony records in climatic reconstruction: a case study from Catalonia (Spain). Clim Change 30:201–221

Masson-Delmotte V, Raffalli-Delerce G, Danis PA, Yiou P, Stievenard M, Giubal F, Mestre O, Bernard V, Goosse H, Hoffmann G, Jouzel J (2005) Changes in European precipitation seasonality and in drought frequencies revealed by a four-century-long tree-ring isotopic record from Brittany, western France. Clim Dynam 24:57–69

Mitchell TD, Jones PD (2005) An improved method of constructing a database of monthly climate observations and associated high-resolution grids. Int J Climatol 25:693–712

New M, Hulme M, Jones PD (2000) Representing twentieth-centruy space-time climate variability. Part II: development of 1901–1996 monthly grids of terrestrial surface climate. J Clim 13:2217–2238

Oberhuber W, Kofler W (2002) Dendroclimatological spring rainfall reconstruction for an inner Alpine dry valley. Theor Appl Climatol 71:97–106

Pauling A, Luterbacher J, Wanner H (2003) Evaluation of proxies for European and North Atlantic temperature field reconstructions. Geophys Res Lett 30:1787–1790, DOI 10.1029/2003GL017589

Pfister C (1999) Wetternachhersage: 500 Jahre Klimavariationen und Naturkatastrophen (1496–1995). Verlag Haupt, Bern, p 304

Pfister C (2005) Weeping in the snow, the second period of little ice age-type impacts. In: Behringer W, Lehmann H, Pfister C (eds) Cultural consequences of the 'Little Ice Age' ('Kulturelle Konsequenzen der Kleinen Eiszeit'), Vandenhoech and Ruprecht, Göttingen, pp 31–86

Proctor CJ, Baker A, Barnes WL, Gilmour MA (2000) A thousand year speleothem proxy record of North Atlantic climate from Scotland. Clim Dynam 16:815–820

Przybylak R, Majorowicz J, Wójcik G, Zielski A, Chorazyczewski W, Marciniak K, Nowosad W, Olinski P, Syta K (2005) Temperature changes in Poland from the 16th to the 20th centuries. Int J Climatol 25:773–791

Qian B, Xu H, Corte-Real J (2000) Spatial-temporal structures of quasi-periodic oscillations in precipitation over Europe, Int J Climatol 20:1583–1598

Rácz L (1999) Climate history of Hungary since 16th century: past, present and future. Centre for Regional Studies of the Hungarian Academy of Sciences, Pécz

Raffalli-Delerce G, Masson-Delmotte V, Dupouey M, Stievenard M, Breda N, Moisselin JL (2004) Reconstruction of summer droughts using tree-ring cellulose isotopes: a calibration study with living oaks from Brittany (western France). Tellus 56:160–174

Raible CC, Casty C, Esper J, Luterbacher J, Pauling A, Rösch AC, Schär C, Tschuck P, Vidale PL, Wild M, Wanner W (2005) Climate variability—observations, reconstructions, and model simulations for the Atlantic-European and Alpine region from 1500 to 2100. Clim Change (in press)

Rimbu N, Lohmann G, Felis T, Pätzold J (2001) Arctic Oscillation signature in a Red Sea coral. Geophys Res Lett 28:2959–2962

Rodrigo FS, Esteban-Parra M, Pozo-Vázquez D, Castro-Díez Y (1999) A 500-year precipitation record in southern Spain. Int J Climatol 19:1233–1253

Rodrigo FS, Pozo-Vázquez D, Esteban-Parra M, Castro-Díez Y (2001) A reconstruction of the winter North Atlantic Oscillation Index back to AD 1501 using documentary data in Southern Spain. J Geophys Res 106:14805–14818

Rodriguez-Puebla C, Encinas AH, Sáenz J (2001) Winter precipitation over the Iberian Peninsula and its relationship to circulation indices. Hydrol Earth Syst Sci 5:233–244

Rutherford S, Mann ME, Osborn TJ, Bradley RS, Briffa KR, Hughes MK, Jones PD (2005) Proxy-based northern hemisphere surface temperature reconstructions: sensitivity to methodology, predictor network, target season and target domain. J Clim 18:2308–2329

Ryan PT (1997) Modern regression methods. Wiley, New York, p 511

Saz MA (2004) Temperaturas y precipitaciones en la mitad norte de España desde el siglo XV. Estudio dendroclimático. Consejo de Protección de la Naturaleza, Diputación General de Aragón, Zaragoza. p294

Schmutz C, Luterbacher J, Gyalistras D, Xoplaki E, Wanner H (2000) Can we trust proxy-based NAO index reconstructions? Geophys Res Lett 27:1135–1138

Slonosky VC, Jones PD, Davies TD (2001a) Instrumental pressure observations and atmospheric circulation from the 17th and 18th centuries: London and Paris. Int J Climatol 21:285–298

Slonosky VC, Jones PD, Davies TD (2001b) Atmospheric circulation and surface temperature in Europe from the 18th century to 1995. Int J Climatol 21:63–75

Slonosky VC, Yiou P (2002) Does the NAO index represent zonal flow? The influence of the NAO on North Atlantic surface temperature. Clim Dynam 19:17–34

Slonosky VC (2002) Wet winters, dry summers? Three centuries of precipitation data from Paris. Geophys Res Lett 29(19):1895, DOI 10.1029/2001GL014302

Steiner D, Pauling A, Nesje A, Luterbacher J, Wanner H, Zumbühl HJ (2005) Sensitivity of European glaciers to precipitation and temperature – two case studies. Clim Dynam (in review)

Strumia G, Wimmer R, Grabner M (1997) Dendroclimatic sensitivity of *Pinus Nigra Arnold* in Austria. Dendrochronologia 15:129–137

Tabony RC (1981) A principal component and spectral-analysis of European rainfall. J Climatol 1:283–294

Tarand A (1993) Precipitation time series in Estonia in 1751–1990. Zeszyty Naukowe Uniwersytetu Jagiellonskiego, Prace Geograficzne:139–149

Till C, Guiot J (1990) Reconstruction of precipitation in Morocco since 1100 AD based on Cedrus atlantica tree-ring widths. Quaternary Res 33:337–351

Timm O, Ruprecht E, Kleppek S (2004) Scale-dependent reconstruction of the NAO index. J Clim 17:2157–2169

Touchan R, Meko D, Hughes MK (1999) A 396-year reconstruction of precipitation in southern Jordan. J Am Water Resour As 35(1):49–59

Touchan R, Garfin GM, Meko DM, Funkhouser G, Erkan N, Hughes MK, Wallin BS (2003) Preliminary reconstructions of spring precipitation in southwestern Turkey from tree-ring width. Int J Climatol 23:157–171

Touchan R, Xoplaki E, Funkhouser G, Luterbacher J, Hughes MK, Erkan N, Akkemik Ü, Stephan J (2005) Reconstructions of spring/summer precipitation for the Eastern Mediterranean from tree-ring widths and its connection to large-scale atmospheric circulation. Clim Dynam 25:75–98

Turkes M (1996) Spatial and temporal analysis of annual rainfall variations in Turkey. Int J Climatol 16:1057–1076

Turkes M (1998) Influence of geopotential heights, cyclone frequency and southern oscillation on rainfall variations in Turkey. Int J Climatol 18:649–680

Turkes M, Erlat E (2003) Precipitation changes and variability in Turkey linked to the North Atlantic Oscillation during the period 1930–2000. Int J Climatol 23:1771–1796

Van Loon H, Rogers HJ (1978) The seesaw in winter temperatures between Greenland and Northern Europe. Part I: general description. Mon Weather Rev 106:296–310

Von Storch H, Zorita E, Cubasch U (1993) Downscaling of global climate change estimates to regional scales: an application to Iberian rainfall in wintertime. J Climate 6:1161–1171

Wanner H et al (2004) Dynamic and socioeconomic aspects of historical floods in central Europe. Erdkunde 58:1–16

Wanner H, Brönnimann S, Casty C, Gyalistras D, Luterbacher J, Schmutz C, Stephenson DB, Xoplaki E (2001) North Atlantic Oscillation—concepts and studies. Surv Geophys 22:321–381

Wanner H, Gyalistras D, Luterbacher J, Rickli R, Salvisberg E, Schmutz C (2000) Klimawandel im Schweizer Alpenraum. vdf Verlag, Zürich, p 285

Wilks DS (1995) Statistical methods in the atmospheric sciences: an introduction. Academic Press, London

Wilson R, Luckman BH, Esper J (2005) A 500-year dendroclimatic reconstruction of spring/summer precipitation from the Lower Bavarian Forest region, Germany. Int J Climatol 25:611–630

Wales-Smith B (1971) Monthly and annual totals of rainfall representative of Kew, Surrey, from 1697 to 1970. Meteorol Mag 100:345–362

Wigley TML, Lough JM, Jones PD (1984) Spatial patterns of precipitation in England and Wales and a revised, homogenous England and Wales precipitation series. J Climatol 4:1–25

Xoplaki E, Gonzalez-Rouco JF, Luterbacher J, Wanner H (2004) Wet season Mediterranean precipitation variability: influence of large-scale dynamics and trends. Clim Dynam 23:63–78

Xoplaki E, Luterbacher J, Burkard R, Patrikas I, Maheras P (2000) Connection between the large scale 500 hPa geopotential height fields and precipitation over Greece during wintertime. Clim Res 14:129–146

Xoplaki E, Luterbacher J, Paeth H, Dietrich D, Steiner N, Grosjean M, and Wanner H (2005) European spring and autumn temperature, variability and change of extremes over the last half millennium. Geophys Res Lett 32:L15713, DOI 10.1029/2005GL023424

Xoplaki E, Maheras P, Luterbacher J (2001) Variability of climate in meridional Balkans during the periods 1675–1715 and 1780–1830 and its impact on human life. Clim Change 48:581–615

Zorita E, Kharin V, von Storch H (1992) The atmospheric circulation and sea surface temperature in the North Atlantic area in winter: their interaction and relevance for Iberian precipitation. J Clim 5:1097–1108

Zveryaev II (2004) Seasonality in precipitation variability over Europe. J Geophys Res 109 D05103, DOI 10.1029/2003JD003668